Universidade de Aveiro Secção Autónoma das Ciências da Saúde
2014

Sara Margarida Leonardo de Oliveira

Produzir e Testar Ferramentas de Biologia Molecular para a PP1

Produce and Test PP1 Molecular Biology Tools

Universidade de Aveiro Secção Autónoma das Ciências da Saúde
2014

Sara Margarida Leonardo de Oliveira

Produzir e Testar Ferramentas de Biologia Molecular para a PP1

Produce and Test PP1 Molecular Biology Tools

Dissertação apresentada à Universidade de Aveiro para cumprimento dos requisitos necessários à obtenção do grau de Mestre em Biomedicina Molecular, realizada sob a orientação científica da Professora Doutora Sandra Maria Tavares da Costa Rebelo, Professora Auxiliar Convidada da Secção Autónoma das Ciências da Saúde da Universidade de Aveiro.

Este trabalho contou com o apoio do centro de biologia celular (CBC) da Universidade de Aveiro, e é financiado por fundos FEDER através do Programa Operacional Factores de Competitividade – COMPETE e por Fundos nacionais da FCT – Fundação para a Ciência e Tecnologia no âmbito do projeto PTDC/BEX-BCM/0493/2012 e PEst-OE/SAU/UI0482/2014.

o júri

presidente

Prof. Doutora Odete Abreu Beirão da Cruz e Silva
Professora Auxiliar com agregação da Secção Autónoma das Ciências da Saúde da Universidade de Aveiro

Doutora Tânia Isabel Sousa Caetano
Estagiária em Pós-doutoramento do Centro de Estudos do Ambiente e do Mar (CESAM) da Universidade de Aveiro (arguente)

Prof. Doutora Sandra Maria Tavares da Costa Rebelo
Professora Auxiliar Convidada da Secção Autónoma das Ciências da Saúde da Universidade de Aveiro

agradecimentos

À Professora Doutora Sandra Rebelo, pela orientação, apoio, conhecimentos partilhados, empenho, motivação e optimismo. Muito obrigada!

À Professora Doutora Odete da Cruz e Silva, pela oportunidade de desenvolver esta dissertação e de trabalhar no Laboratório de Neurociências.

Ao Centro de Biologia Celular da Universidade de Aveiro e à FCT.

A todos os meus colegas dos Laboratórios de Neurociências, Organelle Dynamics in Infection and Disease e Transdução de Sinais. Obrigada pelo apoio, amizade, brincadeiras e momentos de convívio. Um obrigada muito especial à Filipa, por todo o apoio, dedicação, conselhos, ensinamentos e paciência! À Joana Serrano, pela força, entusiasmo, ideias e brincadeiras! À Mónica, pela simpatia, disponibilidade, paciência e partilha de conhecimentos!

Aos meus colegas e amigos de mestrado, Cátia, Sandra, Rita, Daniel, Cláudia, Sílvia, Inês Pinheiro e Christian, por toda a alegria, brincadeiras, distração e entreajuda, jantares, almoços e lanches. Muito obrigada pela amizade que torna tudo muito melhor!

À Simas, Rita e Inês, pela grande amizade que se mantém, apesar de termos seguido caminhos diferentes!

Às minhas grandes e sempre amigas, Inês, Teresa, Beatriz, Mariana, Betty e Mafalda. Mesmo longe, sempre presentes!

A todos os meus amigos, muito obrigada por tudo!

À minha família, Avó Mila e Avô Leonardo, Mã e Miguel, Nelinha, Fernando e Pedro, pelo amor incondicional, apoio e por acreditarem em mim sempre!

palavras-chave

Fosforilação de proteínas, proteína fosfatase 1, silenciamento de genes, shRNA, *constructs* fluorescentes

resumo

A proteína fosfatase 1 (PP1) é uma proteína fosfatase específica para resíduos de serina e treonina que apresenta elevados níveis de expressão no cérebro. A PP1 está envolvida em vários processos biológicos e cascatas de sinalização e a sua função é determinada pela ligação da subunidade catalítica da PP1 com várias subunidades reguladoras (PIPs). Esta interação é mediada através de sequências de aminoácidos específicas designadas de motivos de ligação à PP1, como o motivo RVxF. As isoformas da PP1 são codificadas por três genes: *PPP1CA*, *PPP1CB* e *PPP1CC* que codificam a PP1alfa, PP1beta/delta e PP1gama. O último sofre *splicing* alternativo e origina as isoformas PP1gama1 e PP1gama2. Estas isoformas diferem nos domínios N- e C-terminal e apresentam distribuição tecidual e localização subcelular distintas. Estudos recentes realizados no nosso laboratório demonstraram que as proteínas BRI2 e BRI3, membros de uma família de glicoproteínas integrais transmembranares tipo II, interagem com a PP1 e confirmaram a presença de motivos RVxF em ambas as proteínas, KVTF e KISF para a BRI2 e BRI3, respectivamente. *Short hairpin RNA* (shRNA) é uma forma de RNA de interferência (RNAi) produzido artificialmente que consiste numa pequena sequência de DNA de cadeia dupla com um *hairpin loop* e que utiliza a maquinaria da célula hospedeira para silenciar ou provocar *knockdown* de genes específicos através da degradação da sequência de RNA mensageiro, impedindo assim a tradução. *Knockdown* das proteínas humanas PP1alpha e PP1gamma foi induzido em células de neuroblastoma humanas através da estratégia de shRNA de interferência, para mimetizar o comportamento da célula na ausência de PP1alpha e PP1gamma e para observar os seus efeitos na expressão das proteínas BRI2 e BRI3. O procedimento de transfeção foi optimizado e, através de *immunoblotting*, concluímos que a melhor eficiência de interferência foi obtida 48 horas após transfeção de 3.5 µg de DNA, com TurboFect. Novamente por *immunoblotting*, verificámos que o knockdown da PP1alfa e PP1gamma poderá interferir no processamento da BRI2 e BRI3. Adicionalmente, foram produzidos, através de *PCR subcloning*, *constructs* fluorescentes das isoformas PP1alpha e PP1gamma1 utilizando o vector DsRed-Monomer. Estes *constructs* serão particularmente importantes para estudos futuros *in vivo* para caracterização dos complexos PP1:BRI.

keywords Protein phosphorylation, protein phosphatase 1, gene silencing, shRNA, fluorescent constructs

abstract Protein phosphatase 1 (PP1) is an ubiquitously expressed serine/threonine protein phosphatase with high expression levels in brain. PP1 is involved in many biological processes and signalling pathways and its specific function is determined by the binding of PP1 catalytic subunit to many regulatory subunits, called PP1 interacting proteins (PIPs). This interaction is mediated through specific amino acid sequences, the PP1 binding motifs, as RVxF motif. PP1 is encoded by three different genes: *PPP1CA*, *PPP1CB* and *PPP1CC* that encode PP1alpha, PP1beta/delta and PP1gamma. The later undergoes alternative splicing to give rise to PP1gamma1 and PP1gamma2. These isoforms differ in the C- and N-terminal domains and have distinct tissue distribution and subcellular localization. Recent data from our laboratory established both BRI2 and BRI3, members of a family of integral type II transmembrane glycoproteins, as PIPs and confirmed the presence of RVxF motifs in both proteins, KVTF and KISF for BRI2 and BRI3, respectively. Short hairpin RNA (shRNA) is a form of Ribonucleic acid interference (RNAi) artificially produced that consists of a small sequence of double stranded DNA with an hairpin loop and uses host machinery to silence or knockdown specific genes through degradation of its mRNA sequence, thereby preventing its translation. Knockdown of human PP1alpha and PP1gamma was induced in human neuroblastoma cells, through shRNA interference strategy in order to mimic the cellular behaviour in the absence of PP1alpha and PP1gamma and observe its effects on BRI2 and BRI3 expression. The transfection procedure was optimized and, through immunoblotting, we concluded that the best interference efficiency was obtained at 48 hours upon transfection of 3.5 µg of DNA using TurboFect reagent. Once more through immunoblotting, we verified that PP1alpha and PP1gamma knockdown might interfere with BRI2 and BRI3 processing. Additionally, fluorescent constructs of PP1alpha and PP1gamma1 isoforms were generated through PCR subcloning, using DsRed-Monomer vector. These constructs will be particularly important for future *in vivo* studies for the characterization of PP1:BRI complexes.

Index

Index of Figures

Index of Tables

Abbreviations

AA	Antibiotic/Antimycotic
aa	Amino acid
Ago	Argonaute protein
APS	Ammonium Persulfate
ADAM-10	A Disintegrin and Metalloproteinase Domain 10
ADP	Adenosine Diphosphate
ATP	Adenosine Triphosphate
BCA	Bicinchoninic Acid
BSA	Bovine Serum Albumin
Bp	Base pairs
DGCR8	DiGeorge Syndrome Critical Region Gene 8
DMEM	Dulbecco's Modified Eagle's Medium
DNA	Deoxyribonucleic Acid
dsRNA	Double-Stranded Ribonucleic Acid
E. coli	*Escherichia coli*
FBD	Familial British Dementia
FBS	Fetal Bovine Serum
FCP	TFIIF-associating C-terminal Domain Phosphatase
FDD	Familial Danish Dementia
GFP	Green Fluorescent Protein
GC	Guanine-Citosine content
HBSS	Hank's Balanced Salt Solution
HRP	Horseradish Peroxidase
ICD	Intracellular Domain

LB	Loading Buffer
LB medium	Luria-Bertani medium
LGB	Lower Gel Buffer
MCS	Multiple Cloning Site
MEM	Minimal Essential Medium
MM	Molecular Marker
mRNA	Messenger Ribonucleic Acid
MSC	Missense Control
MT	Melting Temperature
MYPT1	Myosin Phosphatase Targeting Subunit 1
NIPP1	Nuclear Inhibitor of PP1
NTC	Non-Transfected Control
NTF	N-Terminal Fragment
PACT	PKR Activating Protein
PBS	Phosphate Buffered Saline
PCR	Polymerase Chain Reaction
PIP	PP1 Interacting Protein
PK	Protein Kinase
PKR	RNA-dependent Protein Kinase
PP	Protein Phosphatase
PP1	Protein Phosphatase 1
PP1c	Protein Phosphatase 1 catalytic subunit
pri-shRNA	Primary shRNA Transcript
Ran	Ras related GTPase
RE	Restriction Enzyme
RISC	RNA-Induced Silencing Complex

RLC	RISC Loading Complex
RNAi	Ribonucleic Acid interference
rpm	Rotation per minute
SCD	Small C-terminal Domain Phosphatase
SDS	Sodium Dodecyl Sulphate
SDS-PAGE	Sodium Dodecyl Sulphate-Polyacrylamide Gel Electrophoresis
SEM	Standard Error of the Mean
siRNA	Small Interfering Ribonucleic Acid
shRNA	Short Hairpin Ribonucleic Acid
SPPL2a/2b	Signal Peptide Peptidase-Like protease 2a/2b
ssRNA	Single-Stranded Ribonucleic Acid
STPP	Serine/Threonine-specific Protein Phosphatase
TAE buffer	Tris-Acetate-EDTA buffer
TBS	Tris-Buffered Saline solution
TBST	Tris-Buffered Saline solution with Tween detergent
TEMED	N, N, N', N'-Tetramethylethylenediamine
TM	Transmembrane Domain
TRBP	Tat-RNA-Binding Protein
UGB	Upper Gel Buffer
WR	Working Reagent

1. Introduction

1.1. Protein Phosphorylation and Protein Phosphatases

Protein phosphorylation is an important reversible post-translational modification in eukaryotic cells that regulates several and diverse cellular processes such as neurotransmission, muscle contraction, T-cell activation, cell proliferation, signalling, differentiation, metabolic processes, transport and secretory processes, cell adhesion (Cruz e Silva *et al.* 1995; Aggen *et al.* 2000; Barford *et al.* 1998; Hunter 1995). The phosphorylation level of a specific protein is meticulously controlled by protein kinases (PKs) and protein phosphatases (PPs) and it is necessary a delicate balance between their activities, otherwise, alterations in protein phosphorylation levels of target proteins can occur and cause several pathological conditions and/or cellular dysfunctions. Protein kinases covalently transfer phosphate groups from ATP to a specific protein, while the protein phosphatases remove it, as represented in Figure 1 (Ceulemans and Bollen 2004; Barford *et al.* 1998; Hunter 1995). Protein phosphorylation occurs mainly in three hydroxyl-containing residues: serine, threonine and tyrosine. Curiously, approximately one-third of all eukaryotic proteins are regulated by protein phosphorylation on those residues. Protein kinases and phosphatases can be specific for either tyrosine residues or serine and threonine residues (Fardilha *et al.* 2010; Gallego and Virshup 2005; Shi 2009; Sugiyama *et al.* 2012).

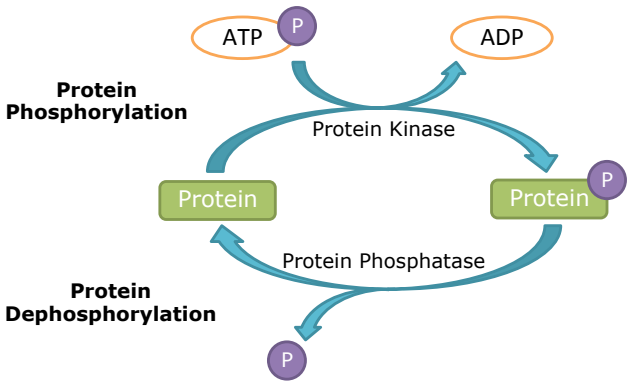

Figure 1 Schematic representation of reversible protein phosphorylation. Protein kinases transfer a phosphate group from ATP to the target protein (protein phosphorylation), while protein phosphatases catalyse the hydrolysis of the phosphate group (P) from the target protein (protein dephosphorylation). *ADP, adenosine diphosphate; ATP, adenosine triphosphate.*

In the human genome, contrary to what would be expected given the remarkable specificity of signalling and the reversible nature of protein phosphorylation, there are more kinases than phosphatases. The number of tyrosine kinases, approximately one hundred, equals the number of tyrosine-specific protein phosphatases (TPP) family. This family includes tyrosine-specific PPs and

double-specificity PPs that are able to dephosphorylate both serine/threonine and tyrosine residues (Fardilha *et al.* 2010; Gallego and Virshup 2005; Shi 2009). In contrast, the number of approximately forty five serine/threonine-specific protein phosphatases (STPPs) is considerably lower than the number of serine/threonine protein kinases, approximately four hundred (Sugiyama *et al.* 2012; Bollen *et al.* 2010). This discrepancy can be explained by the unique manner by which serine/threonine protein phosphatases are regulated. These enzymes have additional interacting and regulatory proteins that bind to the phosphatase catalytic subunit and control their activity and/or subcellular localization (Cruz e Silva *et al.* 1995; Gallego and Virshup 2005; Shi 2009). Serine/threonine-specific protein phosphatases regulate important biological processes: early embryonic development, cell proliferation, cell death, circadian rhythm and cancer (Gallego and Virshup 2005).

Based on substrate specificity, eukaryotic protein phosphatases can be classified into two families: serine/threonine protein phosphatases that catalyse the dephosphorylation of serine and threonine residues and tyrosine phosphatases that catalyse the dephosphorylation of tyrosine amino acids (aa). Serine/threonine protein phosphatases can be divided into three major protein families, structurally unrelated: metal-dependent protein phosphatases (PPMs), aspartate-based phosphatases represented by FCP/SCP (TFIIF-associating C-terminal domain (CTD) phosphatase/small CTD phosphatase) and phosphoprotein phosphatases (PPPs). PPM encodes PPs, which are Mn^{2+}/Mg^{2+} dependent enzymes, like PP2C and pyruvate dehydrogenase phosphatase. These proteins have domains and conserved motifs that help determine substrate specificity and do not have additional regulatory subunits like PPPs. FCP/SCP gene family codifies proteins specific for RNA polimerase II substrate, like FCP1 and SCPs 1-3 (Gallego and Virshup 2005; Shi 2009; Ceulemans and Bollen 2004). Members of the last gene family, PPPs, include: PP1, PP2A, PP2B (also known as calcineurin), PP4, PP5, PP6 and PP7. PP1 and PP2A are some of the most well conserved enzymes with a variety of cellular functions attributed to the interaction with a large number of regulatory subunits (reviewed in Shi 2009; Honkanen and Golden 2002; Moorhead et al. 2009). PP2B alone is inactive, acquiring phosphatase activity upon binding with Ca^{2+}. In sharp contrast, PP1 and PP2A are mainly active in the absence of divalent cations, despite dephosphorylation of some substrates being strongly stimulated by Mn^{2+} (Cohen 1989; Wang *et al.* 2008). PP4, PP5 and PP6, like PP1, PP2A and PP2B were identified in all mammalian tissues. Structurally PP4 and PP6 are closely related to the catalytic subunit of PP2A. PP5 contains an N-terminus tetratricopeptide repeat domain that is a protein-protein interaction motif (Shi 2009; Cohen 1997). In contrast to the other PPPs, human PP7 is not ubiquitous and was primarily found

in retina. PP7 contains multiple Ca^{2+} binding sites and its activity is dependent of Mg^{2+} (Kutuzov *et al.* 2002). These PPPs contain a common catalytic core domain that is conserved among species. PP1, PP2A and PP2B together with the PP2C of the PPM family, account for the majority of the serine/threonine phosphatase activity *in vivo* (Barford *et al.* 1998).

1.2. Protein Phosphatase 1

PP1 (Protein Phosphatase 1) is a major serine/threonine protein phosphatase with broad substrate specificity, wide distribution and it is ubiquitously expressed in all eukaryotic cells (Cruz e Silva *et al.* 1995; Bollen *et al.* 2010; Shi 2009). It is the most abundant protein phosphatase and its catalytic subunit has approximately 37 kDa. PP1 study began around 1940 and this enzyme was known for the conversion of phosphorylase a in phosphorylase b. Afterwards it was discovered that PP1 had actually a phosphatase function (Green and Cori 1943; Sutherland and Wosilait 1955). It has been involved in several biological processes such as transcription, RNA processing, translation, cytoskeleton organization, apoptosis, signal transduction pathways, cell division, cell-cycle progression, sperm motility, muscle contraction, lipid and glycogen metabolism (Fardilha *et al.* 2010; Chakrabarti *et al.* 2007). In the brain, PP1 is involved in neuronal signalling, regulation of neurons and information processing, regulation of neurotransmitter receptors, negative regulation of calcium-activated kinase signalling, ion channel modulation, synaptic plasticity and long-term potentiation and depression related to learning and memory (Strack *et al.* 1999).

PP1 holoenzymes are composed by a highly conserved catalytic subunit called PP1 catalytic subunit (PP1c) complexed with one or two variable regulatory subunits. The crystal structure of PP1c revealed that PP1 is a metalloenzyme with two divalent metal ions (Mn^{2+} and Fe^{2+}). These ions are necessary to PP1 activity since they bind and activate the water molecule for the initiation of the nucleophilic attack on the phosphorous atom (Shi 2009; Egloff *et al.* 1995; Barford *et al.* 1998; Ceulemans and Bollen 2004). The PP1c forms a compact alpha/beta fold structure with a beta-sandwich of two mixed beta-sheets surrounded by two alpha-helical domains, one with seven alpha-helices and other with three alpha-helices and three-stranded beta-sheet. This conformation forms a Y-shaped surface groove that encloses the catalytic centre (Shi 2009; Ceulemans and Bollen 2004; Barford *et al.* 1998; Egloff *et al.* 1997). The catalytic active site of PP1 is located in the intersection of three potential substrate-binding grooves: the hydrophobic, the

acidic and the C-terminal grooves (Shi 2009; Peti *et al.* 2012; Ceulemans and Bollen 2004). PP1alpha structure is represented in Figure 2.

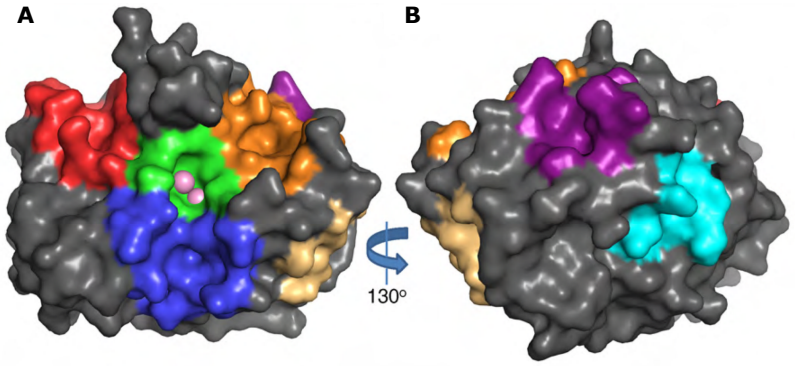

Figure 2 Representation of the PP1alpha structure. A – PP1alpha contains two divalent metal ions (pink spheres) at the centre of the catalyric site (green), which is located at the intersection of three potential substrate-binding grooves: the hydrophobic (blue), the acidic (orange) and the C-terminal (red). **B –** 130° rotation of **A** to show the binding sites for the RVxF (purple), SILK (cyan) and MyPhone (wheat) motifs (Bollen *et al.* 2010).

1.2.1. PP1 Isoforms

In mammals, PP1 isoforms are encoded by three genes: *PPP1CA*, *PPP1CB* and *PPP1CC* that encode for PP1alpha, PP1beta/delta and PP1gamma, respectively (Strack *et al.* 1999; Chakrabarti *et al.* 2007; Peti *et al.* 2012; Ceulemans and Bollen 2004). The gene encoding PP1gamma undergoes alternative splicing to originate an ubiquitous PP1gamma1 and PP1gamma2, a variant testis enriched (Cruz e Silva *et al.* 1995). These isoforms are about 90% identical in amino acid sequence. Most of the differences are located at the N- and C-terminals (Chakrabarti *et al.* 2007; Peti *et al.* 2012; Andreassen *et al.* 1998; Ceulemans and Bollen 2004). PP1alpha, PP1gamma1 and PP1gamma2 are 330, 323 and 337 amino acids long, respectively (Uniprot 2014; NCBIa 2014; NCBIb 2014; NCBIc 2014).

PP1 is an ubiquitous protein but the three isoforms have different tissue distributions and subcellular localizations. PP1alpha is highly expressed in mammalian brain, specifically neurons and neuroglia. PP1gamma1 is also highly expressed in brain and, in rat, it was observed particularly in the striatum and hippocampus. Once it was observed in dendritic spines and in some presynaptic terminals, this isoform probably regulates presynaptic membrane excitability, neurotransmitter synthesis, uptake and release (Strack *et al.* 1999; Cohen 2002b). PP1gamma2 is highly expressed in testis and spermatozoa and regulates sperm motility (Chakrabarti *et al.* 2007; Huang and Vijayaraghavan 2004).

At a subcellular level, localization of endogenous PP1 is not entirely clear but this enzyme is enriched in the nucleus compared to the cytosol and its isoforms have different intranuclear distribution (Ulke-Lemée *et al.* 2007). These differences can be due to different affinities for regulatory subunits with different subcellular distribution. PP1alpha and PP1gamma accumulates in unidentified nuclear bodies and in nucleoli, respectively, and both are diffuse in the cytoplasm and nucleoplasm (Trinkle-Mulcahy *et al.* 2001).

During the cell cycle, localization of PP1 inside the cell changes. During interphase PP1alpha is associated with nuclear matrix and is probably involved in pre-RNA splicing. During mitosis, this isoform is found in centrosomes and it is possibly related to metaphase-anaphase transition and checkpoint mechanisms. PP1gamma1 localizes in the nucleolus during interphase and is associated to microtubules of the mitotic spindle during mitosis. Thereby, in interphase and mitosis, it may be involved in ribosome processing and chromosome segregation, respectively (Andreassen *et al.* 1998).

1.2.2. PP1 Regulation

Interestingly, the catalytic rates, substrate specificity and inhibition profiles, *in vitro*, are similar for all the four catalytic subunit isoforms of PP1. However, in cells, PP1c does not appear alone, but it forms heteromeric complexes with different regulatory subunits instead, called holoenzymes, important to restrain and direct PP1 catalytic activity, preventing widespread dephosphorylation (Ceulemans and Bollen 2004; Strack *et al.* 1999; Lee *et al.* 2010; Gallego and Virshup 2005). The association between PP1 activity and high molecular weight complexes, observed by gel filtration, and subsequent decrease of molecular weight after proteolysis, urea or ethanol treatment, corroborates the formation of holoenzymes complexes (Killilea *et al.* 1979; Mellgren *et al.* 1979). It is estimated that, in mammals, PP1 can form approximately 650 distinct holoenzymes (Bollen *et al.* 2010). A functional PP1 holoenzyme consists of a catalytic subunit and one or more regulatory subunits, which direct PP1 to specific cellular compartments, determining PP1 function with considerable selectivity (Aggen *et al.* 2000; Shi 2009; Meiselbach *et al.* 2006).

Most PP1 regulatory subunits, called PP1 interacting proteins (PIPs), interact with PP1c through a conserved PP1 binding motif termed the RVxF motif. The RVxF motif binds to the hydrophobic groove of PP1c that is distant from the catalytic site (Egloff *et al.* 1995). The residues of PP1c responsible for binding of the RVxF motif are conserved in all isoforms of different species

(Barford *et al.* 1998; Egloff *et al.* 1997). The RVxF motif consists of a short consensus amino acid sequence [K/R] $X_{A(0-1)}$ [V/I] X_B [F/W], where X_A may be absent (0) or any amino acid (1) and X_B is any amino acid except proline (Wakula *et al.* 2003). This is particularly important since the presence of proline prevents beta-strand formation and RVxF adopts this conformation when it binds to PP1c (Gallego and Virshup 2005; Peti *et al.* 2012; Wakula *et al.* 2003). RVxF is present in many other eukaryotic proteins besides PIPs but it is thought that it only works as a PP1 binding motif when it is located in an exposed and flexible loop that can be modelled into a beta-strand (Wakula *et al.* 2003). A remarkable aspect is that the RVxF motif is often N-terminally flanked by basic residues and C-terminally flanked by acidic residues and this affects the binding affinity for the RVxF motif (Meiselbach *et al.* 2006; Wakula *et al.* 2003). The binding of PP1 to regulatory proteins through the RVxF motif causes neither significant conformational changes in PP1c nor major alterations in the phosphatase activity and substrate specificity. Although RVxF motif is necessary and sufficient for the interaction, functioning as an anchor, other low affinity interactions stabilise and strengthen the binding and have regulator-specific effects on PP1 enzymatic activity and substrate specificity (Wakula *et al.* 2003; Ceulemans and Bollen 2004; Peti *et al.* 2012; Meiselbach *et al.* 2006). Therefore, RVxF binding is a prerequisite for the cooperative binding of other motifs that modulate activity and specificity, probably through conformational changes or steric effects in the catalytic site that alters accessibility (Wakula *et al.* 2003; Wakula *et al.* 2006; Cohen 2002b). Mutations in this motif, in the hydrophobic (V/I) or aromatic residue (F/W), disrupt or weaken interaction between PIP and PP1c, which confirms that this is an important site for the interaction. However, with higher concentrations of the interactor protein, the effects in PP1 activity and specificity can still be observed, confirming the role of the secondary lower affinity binding sites (Fardilha *et al.* 2010; Cohen 2002b; Wakula *et al.* 2003).

Additional PP1 binding motifs were identified, the SILK and MyPhone motifs (Figure 2). The SILK motif has the consensus sequence [GS]IL[RK] (Hendrickx *et al.* 2009) and it was first described for inhibitor-2. The SILK motif was shown to be essential for PP1 inhibition by inhibitor-2 (Huang *et al.* 1999) and can functionally replace the RVxF motif in the nuclear inhibitor of PP1 (NIPP1) (Wakula *et al.* 2003). The SILK motif is always positioned N-terminally to the RVxF sequence and binds in a hydrophobic groove on the opposite face of the PP1 active site (Bollen *et al.* 2010). The myosin phosphatase targeting subunit 1 (MYPT1) has a N-terminal PP1 binding motif (MyPhone motif) with the consensus sequence RxxQ[VIL][KR]x[YW], where x can be any residue (Terrak *et al.* 2004). The MyPhone motif is present in other PP1 regulatory proteins and is also N-terminal to the RVxF sequence (Bollen *et al.* 2010).

1.2.3. PP1 Interacting Proteins

More than 200 PIPs have already been identified and they can be classified as targeting proteins, activity regulators (inhibitors or substrate specifiers) or PP1 substrates (Figure 3) although they are often multifunctional (Wakula *et al.* 2003; Ceulemans and Bollen 2004; Meiselbach *et al.* 2006; Peti *et al.* 2012). Targeting proteins can bind to PP1c and one of its substrate or a subcellular structure containing the substrate, so PP1 dephosphorylates a phosphoserine or phosphothreonine residue specifically. Scaffolding proteins that facilitate protein complexes formation are included in this group. The activity regulators can be inhibitors, which block PP1c activity, or substrate specifiers that promote dephosphorylation of specific substrates by PP1c. PP1 substrates bind to the catalytic subunit directly and their controlled dephosphorylation serves a regulatory function, as targeting proteins or activity regulators (Aggen *et al.* 2000; Wakula *et al.* 2003; Bollen *et al.* 2010).

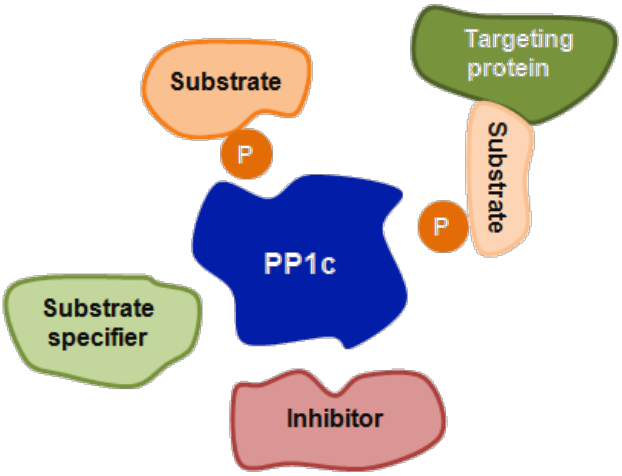

Figure 3 Schematic representation of the PP1 holoenzyme structure. The protein phosphatase 1 catalytic subunit (PP1c) interacts with regulatory subunits that can be substrates, targeting proteins, inhibitors or substrate-specifiers. *PP1c, protein phosphatase 1 catalytic subunit* (Santos 2014).

PIPs bind to PP1c through short PP1 binding motifs but they have multiple sites of interaction with this protein. These interaction sites are identical or overlapping for all PIPs and only one PIP can bind to PP1c at a time, which explains why a relatively small protein as PP1 can interact with numerous different regulatory subunits, structurally unrelated and with different effects on PP1 function, and why the binding of most PIPs is mutually exclusive (Ceulemans and Bollen 2004; Aggen *et al.* 2000; Barford *et al.* 1998). Thus, it is suggested that PP1 is subject to a combinatorial

control that relies on the competition of PIPs for a combination of interaction sites (Ceulemans and Bollen 2004; Fardilha *et al.* 2010; Wakula *et al.* 2003).

Many substrates that directly associate with PP1c are enzymes that are activated by dephosphorylation, as is the case for focal adhesion kinase, E3 ubiquitin ligase and caspase 2 (Bollen *et al.* 2010). In contrast, PP1alpha dephosphorylates NEK2, Aurora-A and C-Nap1 and keeps these proteins in an inactive state (Mi *et al.* 2007). Some substrates are dephosphorylated specifically on a single residue, whereas others are dephosphorylated on multiple residues (Bollen *et al.* 2010). Many PP1 binding proteins mediate the targeting of PP1 to specific subcellular compartments or protein complexes. This brings PP1 in close proximity to specific substrates (Bollen *et al.* 2010; Ceulemans *et al.* 2002). For example, spinophilin directs PP1 to dendritic spines in brain nearby potential substrates which mediate the regulation of PP1 synaptic function (Allen *et al.* 1997). NIPP1 was initially identified as a nuclear inhibitor of PP1c but it also targets PP1 to dephosphorylate spliceosome-associated protein 155 (SAP155), not as an inhibitor of PP1 (Tanuma *et al.* 2008). Some PP1 binding proteins selectively inhibit PP1 dephosphorylation of only a subset of substrates as glycogen phosphorylase. Thus, these proteins are defined as substrate specifiers than as inhibitors. In addition, some substrate specifiers enhance PP1 activity towards PP1 substrates, as is the case of the MYPT1. Interaction of MYPT1 with PP1 not only promotes the dephosphorylation of the myosin regulatory light chain but also decreases PP1 activity towards other substrates (Ceulemans and Bollen 2004; Bollen *et al.* 2010; Bollen 2001). PP1 is inhibited by two small proteins called Inhibitor-1 (I-1) and Inhibitor-2 (I-2). I-1 has 165 aa and molecular mass 23 kDa whereas I-2 has 204 aa and molecular mass 19 kDa. Besides these two inhibitors, there are naturally occurring toxins that powerfully inhibit PPs by binding and occluding the enzyme's catalytic site and hydrophobic groove, such as okadaic acid, calyculin A and tautomycin (Huang and Glinsmann 1976; Holmes *et al.* 1986; Ishihara *et al.* 1989; Mackintosh and Klumpp 1990; Peti *et al.* 2012). The use of PP inhibitors as therapeutic agents does not seem to be a reasonable option. They have broad activity and low or none selectivity and they are involved in several essential cellular processes, which makes them highly toxic to the eukaryotic cells. Contrary to PP inhibitors, it is thought that PIPs would be suitable for therapeutic investigation, as targets, because of the increasing number of proteins involved in different biological processes, with different functions and in different cell types identified as PIPs and consequent PIPs diversity. Therefore, abnormal dephosphorylation, holoenzyme malfunctioning or PIP anomalies can be the cause of many diseases or dysfunctions, as neurodegenerative diseases, infertility and cancer (Fardilha *et al.* 2010).

1.2.4. PP1 Functions

PP1 is the most widely expressed serine/threonine protein phosphatase and regulates a variety of cellular functions. PP1 is involved in glycogen metabolism, transcription, protein synthesis, cellular division and meiosis, and apoptosis. When nutrients are abundant, PP1 stimulates the synthesis of glycogen and also enables the return to the basal state of protein synthesis and the recycling of transcription and splicing factors. PP1 is required for anaphase progression, exit from mitosis and is also responsible for maintenance of the cells in G1 or G2 cell cycle phases. In addition, PP1 can also promote apoptosis when cells are damaged. PP1 in combination with its regulatory proteins is also involved in neurotransmission, neurite outgrowth and synapse formation (reviewed in Ceulemans and Bollen 2004; Cohen 2002a). Most PP1 binding proteins identified so far have an annotated function. In accordance with the broad action of PP1, its binding proteins are also linked to diverse cellular functions. However, they function predominantly in signal transduction events, including regulation of nucleic acid, cell cycle, protein synthesis, stress response, metabolism and transport (Esteves *et al.* 2012; Heroes *et al.* 2013). Despite some PP1 binding proteins do not show cell or tissue-specific expression, others are selectively expressed in brain, testis or white blood cells (Heroes *et al.* 2013), accordingly with the high expression levels of PP1 in those tissues (Cruz e Silva *et al.* 1995; Fardilha *et al.* 2011; Heroes *et al.* 2013). Regarding the subcellular localization, PP1 binding proteins are mainly found in the nucleus, cytoplasm and plasma membrane (Esteves *et al.* 2012; Heroes *et al.* 2013). This is consistent with the fact that all PP1 isoforms can be found in the nucleus and cytoplasm (Andreassen *et al.* 1998).

1.3. BRI Family

BRI gene family comprises at least three members *BRI1/ITM2A*, *BRI2/ITM2B* and *BRI3/ITM2C* that encode for BRI1, BRI2 and BRI3 proteins, respectively. They are a family of integral type II transmembrane glycoproteins with a short cytosolic N-terminal and a large extracellular C-terminal and weight approximately 30 kDa (Vidal *et al.* 2001; Tsachaki *et al.* 2008). The extracellular domain contains a domain called BRICHOS with approximately 100aa. Structurally, these proteins have a single transmembrane domain, a single potential N-glycosylation site and no amino terminal signal peptide (Vidal *et al.* 2001; Choi *et al.* 2001). They have different expression patterns and their physiological function is not well understood (Vidal *et al.* 2001; Rostagno *et al.* 2005). The highest amino acid sequence homology between the three isoforms is

the BRICHOS domain and the C-terminal region (Matsuda *et al.* 2009). It is believed that this is an evolutionarily conserved gene family, since mouse and human genes are homologues (>90% homology, particularly in the C-terminal), and have a similar genomic organization, each gene containing six exons and five introns. The first intron is the longest and therefore may contain regulatory sequences (Choi *et al.* 2001; Rostagno *et al.* 2005).

BRI1, a protein of 263 aa, is expressed in osteogenic and chondrogenic tissues, being involved in osteo- and chondrogenesis, skin and muscle, showing low levels in brain and heart (Vidal *et al.* 2001; Rostagno *et al.* 2005). Regarding the other two family members (BRI2 and BRI3), a more detailed description will be performed since both are new PP1 regulatory proteins and therefore more relevant for this work (Martins et al. 2014, submitted).

1.3.1. BRI2

BRI2 is a highly ubiquitous protein of 266 aa, expressed in all tissues tested so far in human and mouse. However, its highest levels are observed in heart, placenta, kidney and pancreas (Vidal *et al.* 2001; Rostagno *et al.* 2005). It is also ubiquitously expressed in brain, in both white and grey matter but particularly abundant in hippocampus, cerebellum, spinal cord, subthalamic nucleus and substantia nigra. The BRI2 messenger RNA (mRNA) is present in neurons, astrocytes and microglial cells, smooth muscle and cerebral endothelial cells (Rostagno *et al.* 2005; Tsachaki *et al.* 2008).

Although BRI2 function is not well understood, there are evidences that suggest its involvement in several cellular processes. It is thought that BRI2 has a role in transport along neuronal processes and in nerve terminals and synapse, besides its likely participation in neurite outgrowth and possible role in neuronal differentiation (Choi *et al.* 2004; Rostagno *et al.* 2005; Tsachaki *et al.* 2008). It has been observed that in brain regions that suffered ischemia or hypoxia, levels of BRI2 expression are increased, which indicates its implication in neuronal stress pathways. BRI2 has also been proposed as a tumour suppressor gene once it shows, along with other genes of the same locus, significantly reduced levels in prostate tumour, with good correlation with cancer stage and grade (Rostagno *et al.* 2005; Tsachaki *et al.* 2008). Furthermore, BRI2 regulates the processing of Amyloid Precursor Protein (APP), the precursor of Abeta peptide that aggregates to form the Alzheimer's disease characteristic senile plaques. BRI2 inhibits APP cleavage by alpha- and beta-secretases, not by interacting with them directly but by binding to APP and covering the

secretases docking sites, which leads to inhibition of Abeta formation (Tsachaki *et al.* 2008; Matsuda *et al.* 2008).

BRI2 undergoes Regulated Intramembrane Proteolysis (RIP), a two-step proteolytic processing represented in Figure 4: cleavage and secretion of great part of BRI2 ectodomain and intramembrane cleavage. BRI2 is first processed by pro-protein convertase furin and related proteases in the ectodomain, generating a short C-terminal peptide (3 kDa). Then, a disintegrin and metalloproteinase domain 10 (ADAM-10) cleaves the remaining ectodomain, releasing BRICHOS domain (25 kDa) (Ghiso *et al.* 2006; Tsachaki *et al.* 2008; Wickham *et al.* 2005; Martin *et al.* 2008). The remaining membrane-associated N-terminal fragment (NTF) (22 kDa) suffers intramembrane proteolysis by signal peptide peptidase-like proteases 2a or 2b (SPPL2a or SPPL2b) and two fragments are formed, a BRI2 intracellular domain (ICD) (10 kDa), which is released to the cytosol and may mediate signals to the nucleus, and a small secreted BRI2 C-terminal domain (Martin *et al.* 2008; Tsachaki *et al.* 2008; Ghiso *et al.* 2006).

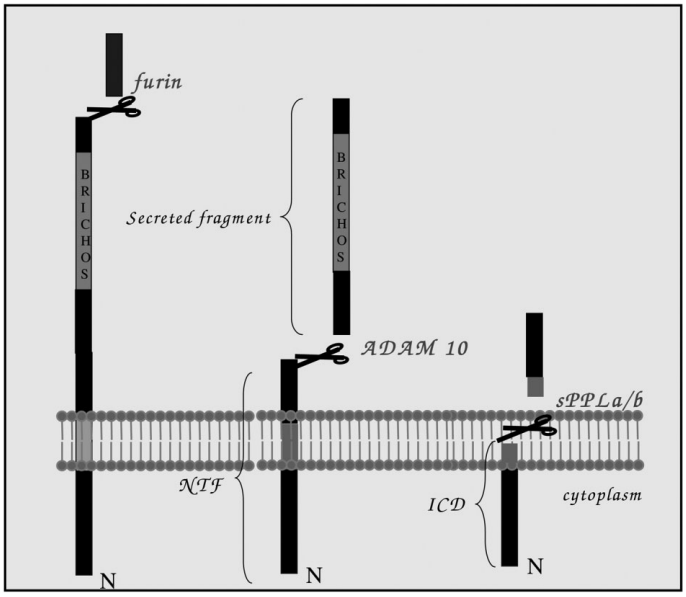

Figure 4 Schematic representation of BRI2 processing. BRI2 is first processed by furin in the ectodomain to release a short C-terminal peptide. Another proteolytic cleavage by ADAM-10 takes place extracellularly, releasing a fragment containing BRICHOS domain. The remaining NTF is cleaved by SPPL2a/2b to form a BRI2 ICD and a small C-terminal domain. *ADAM-10, a disintegrin and metalloproteinase domain 10; ICD, intracellular domain; NTF, N-terminal fragment; SPPL2a/2b, signal peptide peptidase-like proteases 2a and 2b* (Tsachaki *et al.* 2008).

BRICHOS domain is also present in the other two family members: BRI1 and BRI3, as well as in a diversity of proteins implicated in dementia, respiratory distress and cancer. Its secretion was verified in BRI2 but not in the other two members of the BRI family. Its function is unclear but it

may have a role in the extracellular space, probably far from its producing cell (Martin *et al.* 2008; Wickham *et al.* 2005). It has also been suggested an involvement in targeting proteins to the secretory pathway or intracellular protein processing (Rostagno *et al.* 2005; Tsachaki *et al.* 2008).

Mutations in BRI2 gene are associated with two hereditary conditions: Familial British Dementia (FBD) and Familial Danish dementia (FDD) commonly designated Chromosome 13 Dementias. These dementias are characterized by neurodegeneration and extensive amyloid deposition in the central nervous system, particularly with vascular and perivascular localization (Vidal *et al.* 2001; Rostagno *et al.* 2005).

FBD is caused by a point mutation at stop-codon of BRI2 gene turning it into an arginine codon and FDD results from a 10-nucleotide duplication just before the stop-codon. In both cases, a longer precursor will be formed with abnormal C-terminal. After the BRI2 proteolytic process described above, where furin or related proteases cleave BRI2 ectodomain, 34-residues long amyloid subunits will be released and will accumulate in the brain: ABri in the case of FBD and ADan in the case of FDD. The two amyloid proteins share 100% homology in their first 22 residues but have different 12-amino acids C-terminal segment. FBD and FBB cause similar but not identical brain injuries thus, it is most likely that the C-terminal sequence determines amyloid peptides biochemical properties, aggregation, deposition and consequent neuronal dysfunction (Rostagno *et al.* 2005; Vidal *et al.* 2001; Ghiso *et al.* 2006; Choi *et al.* 2004).

Recent data from our laboratory established BRI2 as a novel PP1 regulatory protein and, in fact, *in silico* results revealed that an RVxF PP1 binding motif was found in BRI2 intracellular domain, KVTF (Martins et al. 2014, submitted).

1.3.2. BRI3

BRI3, a 267 aa protein, is mainly expressed in brain, with highest levels in cerebral cortex, medulla, amygdala, hippocampus, thalamus, caudate nucleus and spinal cord (Vidal *et al.* 2001; Rostagno *et al.* 2005). It has also been found in plasmacytoid dendritic cells, granulocytes, bone marrow, fetal liver, and, to lesser extend in spleen, lymph nodes and thymus (Rostagno *et al.* 2005; Ghiso *et al.* 2006). Since it is highly expressed in brain, BRI3 may be implied in maintenance of adult brains and formation of embryonic brains (Choi *et al.* 2001). BRI3, like BRI2, physically interacts with APP and inhibits APP processing by secretases thus reducing Abeta production.

Based on an observed co-localization of BRI3 and APP in vesicles along the neurites, it was proposed that BRI3 might regulate APP processing during its transport through these structures. Dysfunctions on APP processing by BRI2 but most likely by BRI3, once it is predominantly neuronal, may contribute to Alzheimer's disease pathogenesis (Matsuda *et al.* 2009).

Similarly to what happens in the beginning of BRI2 proteolysis (Figure 4), BRI3 is cleaved by a furin in its ectodomain and a 3 kDa C-terminal peptide is secreted. However, although BRI3 is highly homologous to BRI2, it seems to fail both processing by ADAM-10 and intramembrane proteolysis by SPPL2a/2b. Hence, BRICHOS domain is not liberated (Wickham *et al.* 2005).

Recent data from our laboratory established BRI3 as a novel PP1 regulatory protein and, in fact, *in silico* results revealed that an RVxF PP1 binding motif was found in BRI3 intracellular domain, KISF (Martins et al. 2014, submitted).

1.4. RNA Interference Strategy

Cells possess a natural specific and selective mechanism for gene silencing or knockdown denominated Ribonucleic Acid Interference (RNAi) whereby a double-stranded RNA (dsRNA) post-transcriptionally silences the expression of a gene highly homologous to its own sequence (Hannon and Conklin 2004; Scherr and Eder 2007). It is an ancient and evolutionary conserved mechanism that regulates expression of cellular genes and protects the genome against viruses and other mobile genetic elements, preventing its replication, viral infection and genomic instability, by degradation of specific mRNA (Scherr and Eder 2007; Elbashir *et al.* 2001; Nykänen *et al.* 2001; Bernstein *et al.* 2001). RNAi was tested in the nematode worm *Caenorhabditis elegans* using antisense and sense strands to silence a targeted mRNA. However, dsRNA proved to be more effective than single-stranded RNA (ssRNA) as inducer of gene silencing, causing a significant decrease in the level of the target mRNA. Further studies confirmed the presence of RNAi in a variety of organisms such as *Drosophila*, zebrafish and mammals (Paddison *et al.* 2002; Scherr and Eder 2007; Zhou *et al.* 2010).

RNAi mechanism can be briefly explained in two steps, the initiator and the effector. In the initiator step, dsRNA is recognized and cleaved by Dicer enzyme (a member of the RNAse III family of dsRNA-specific ribonucleases) into a small interfering RNA (siRNA). The cleavage of the dsRNA is dependent of ATP, generating 19 to 21 basepairs siRNA duplexes with a 3' overhang of two

nucleotides. In the effector step, siRNA joins a multicomponent nuclease complex and forms RNA-Induced Silencing Complex (RISC), which destroys mRNAs recognized as siRNA homologues (Paddison *et al.* 2002; Hammond *et al.* 2001a; Hammond *et al.* 2001b). The later complex binds to the substrates through their homology to siRNA by base pairing. The mRNA is targeted for destruction through its cleavage at approximately 12 nucleotides from 3' end of the siRNA, resulting in gene-specific knockdown (Paddison *et al.* 2002; Hutvágner and Zamore 2002; Nykänen *et al.* 2001).

In plants and invertebrates, siRNA is able to amplify its effect functioning as a primer for an RNA-dependent RNA polymerase that synthetises additional dsRNA, which is processed into siRNA (Yu *et al.* 2002). In mammalian cells, dsRNAs with more than 30 nucleotides activate an antiviral response that causes non-specific degradation of mRNA and stops protein translation. An alternative to this problem emerged when 21-nucleotide siRNA was synthetized in vitro, introduced in cells and successfully provoked gene-specific suppression, avoiding host responses (Sui *et al.* 2002). Still, commonly used short-hairpin RNA (shRNA) constructs, supposedly too short to induce interferon expression, can cause unwanted responses like interferon-mediated activation of signalling pathways. Interferons are cytokines released by the host cells as the first line of defence against viral infection. Thus, it is recommended the use of the lowest effective shRNA dose, in order to minimize the risk of interferon response, and a careful interpretation of the results obtained from RNAi technology experiments, since shRNA may produce broad effects, decreasing its selectivity (Bridge *et al.* 2003; Sledz *et al.* 2003).

RNAi has been widely used in research, for instance in the determination of gene functions or identification of cellular targets for specific intervention. Moreover, its use in clinical settings is growing due to its therapeutic potential (Scherr and Eder 2007; Yi *et al.* 2005).

RNA interference can be achieved by two different interfering RNAs, siRNA and shRNA, with distinct molecular mechanisms of action, RNA interference pathways, off-target effects and applications (Rao *et al.* 2009a; Rao *et al.* 2009b). siRNA is, as described above, an intermediate in RNAi pathway, and it can be found naturally in the cytoplasm or it can be synthetized and introduced in cells. Despite succeeding in selectively supressing gene expression in cultured mammalian cells without non-specific responses, siRNA silencing lasts only a few days because of its transient nature and the lack of amplification machinery in mammalian cells similar to the existent in *C. elegans* that triggers and keeps gene silencing. To obtain effective knockdown, it would be necessary a higher amount of siRNA, which could contribute to off-target effects. shRNA

is formed in the cell nucleus from a DNA construct previously produced. This DNA vector-based RNAi allows continuous synthesis of shRNA causing a much more durable effect with a smaller dosage and less off-target effects when comparing with siRNA (Rao *et al.* 2009b; Scherr and Eder 2007; Hannon and Conklin 2004; Rao *et al.* 2009a).

1.4.1. shRNA

Short-Hairpin RNA is a form of RNAi artificially produced and consists of 5 bases for the restriction site at the 5' end and one for restriction at the 3' end, 19 bases of sense strand and other 19 of antisense strand. Accordingly, the shRNA contains a perfect double stranded with one of them identical to the target mRNA and another ensuring proper orientation for correct hairpin loop formation. The hairpin loop sequence is composed by 7 to 9 bases linking both strands, in which the most effective is 5'-TTCAAGAGA-3'. After that, there are 6 bases of terminator and, eventually, other 6 of unique restriction site, which allows the restriction digestion analysis to confirm the presence of the cloned insert (Figure 5). Thereby, the result is an oligonucleotide of 63 to 65 basepairs (Paddison *et al.* 2002; Scherr and Eder 2007; Paul *et al.* 2002; Sui *et al.* 2002).

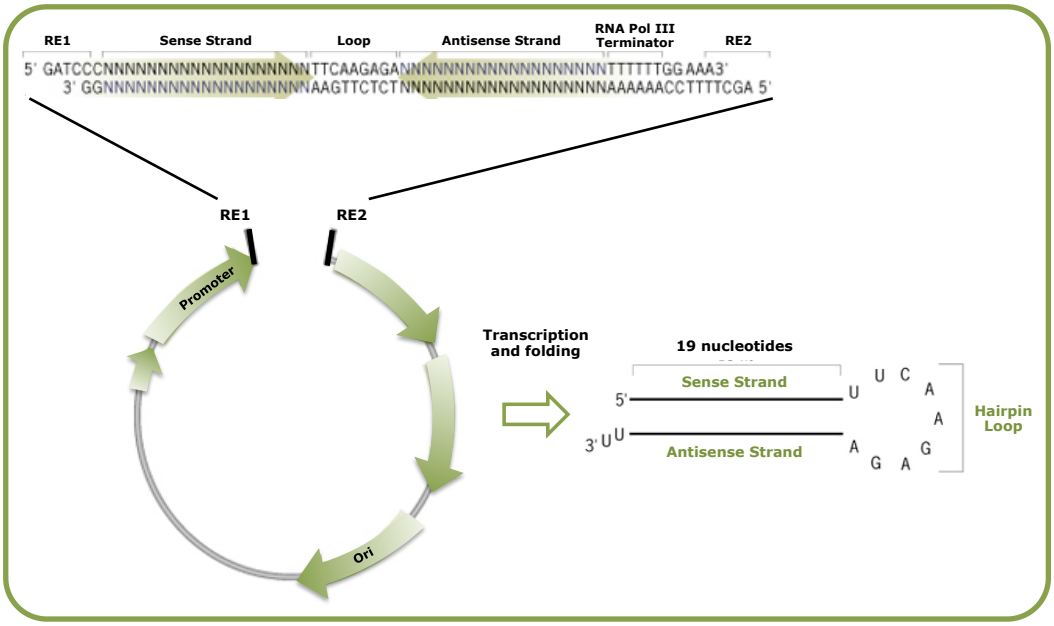

Figure 5 Schematic representation of an shRNA oligonucleotide. Firstly, the DNA target sequence is chosen. Next, the designed oligonucleotide is inserted into the vector, which is delivered into the host cell. The shRNA is transcribed and folds into a loop structure. *RE1/2, restriction enzyme 1 and 2; shRNA, short-hairpin RNA* (adapted from Life Technologies 2014).

Once complete the construction, the vectors contain a DNA sequence that encodes the shRNA cloned between a Polymerase III promoter, like the human U6 promoter, and the transcription termination site. These vectors represent a definite improvement in initiating RNAi, as they use the cell's RNA polymerase III enzyme to transcribe the previously designed shRNA. The human U6 promoter provides high levels of expression in numerous cell types, resulting in target gene knockdown (Kunkel and Pederson 1989). The transcript is terminated at position 2 of the terminator and folds subsequently into a loop structure with 3' overhangs. The shRNA terminations are processed *in vivo*, converting it into twenty one nucleotide siRNA-like molecules, which in turn trigger the RNA interference (Brummelkamp *et al.* 2002).

The DNA vector is introduced in the cell by transfection or infection (Hannon and Conklin 2004; Moore *et al.* 2010) (Figure 6A) and is delivered to the nucleus where it integrates the cell DNA and undergoes transcription, which can be initiated by RNA polymerase II or III through RNA polymerase II or III promoters on the shRNA expression cassete (Rao *et al.* 2009b). The primary shRNA transcript (pri-shRNA) that possesses an hairpin loop (Figure 6B), is cleaved in the nucleus by Drosha, an RNAse III, with help of DiGeorge syndrome critical region gene 8 (DGCR8), a dsRNA binding protein, resulting in the formation of long double-stranded pre-shRNA, ready to be exported to the cytoplasm through a Ran-GTP-dependent mechanism and interaction with endogenous Exportin 5 (Figure 6C) (Rao *et al.* 2009b).

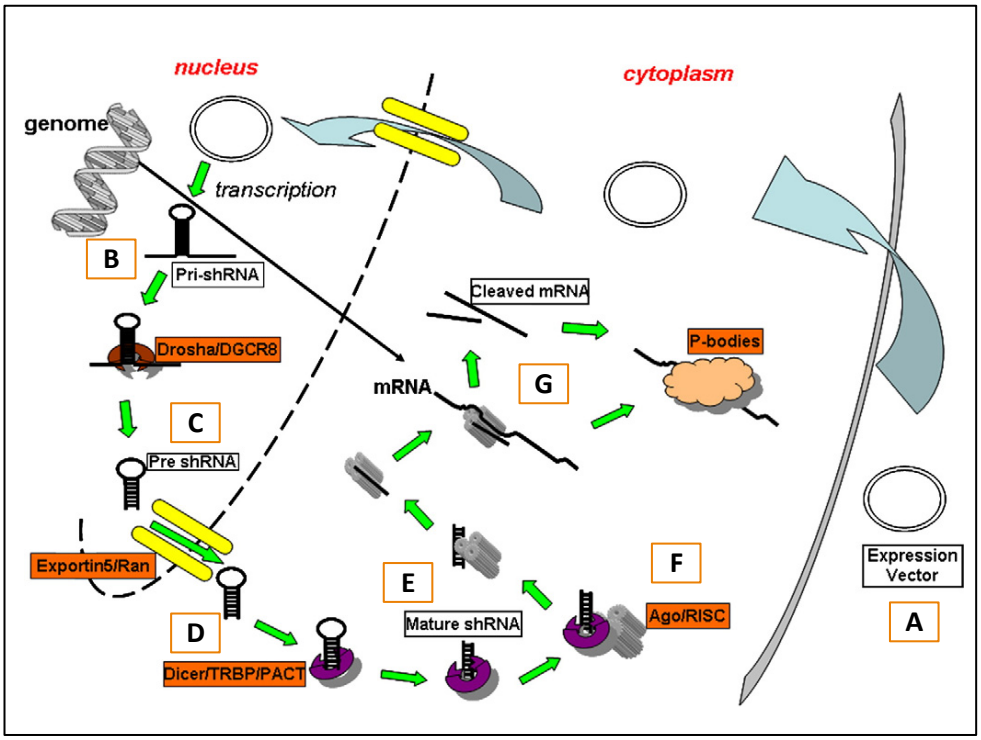

Figure 6 Schematic representation of shRNA interference mechanism. shRNA expression vector is delivered to the cytoplasm (A) and then it is transported to the nucleus, where it is transcribed. The primary shRNA transcripts (B) are processed by Drosha/DGCR8 to form pre-shRNAs (C). Pre-shRNAs are exported to the cytoplasm by Exportin5 and join Dicer/TRBP/PACT complex (D), where mature shRNAs are formed (E). This complex associates with Ago containing RISC and provide RNA interference via target mRNA cleavage and degradation in p-bodies. *Ago, Argonaute protein; DGCR8, DiGeorge syndrome critical region gene 8; PACT, PKR activating protein; Pri-shRNA, primary shRNA transcript; RISC, RNA-induced silencing complex; TRBP, Tat-RNA-binding protein* (adapted from Rao *et al.* 2009b).

In the cytoplasm, when Ran hydrolyzes GTP into GDP, pre-shRNA is free to join the complex formed by RNAse III Dicer, Tat-RNA-binding protein (TRBP) and PKR activating protein (PACT) (Figure 6D). This complex promotes cleavage of pre-shRNA into mature shRNA, a double-stranded siRNA with 5' phosphate and 3' hydroxyl termini, two nucleotides 3' overhangs and no hairpin loop (Figure 6E) (Moore *et al.* 2010; Yi *et al.* 2005; Rao *et al.* 2009b). These are important structural features essential for RNAi pathway, without which RNAi would not be triggered (Hutvágner and Zamore 2002; Nykänen *et al.* 2001). Aside from pre-shRNA processing, Dicer/TRPB/PACT complex also functions as a platform for RISC assembly. Actually, Dicer requires TRBP for protein stability and RISC assembly, including recruitment of endonuclease Argonaute 2 (Ago2) (Chendrimada *et al.* 2005). Mature shRNA is then incorporated in the Ago2 containing RISC (Figure 6F), forming RISC Loading Complex (RLC). Hence, RLC is composed of at least shRNA, Ago2, Dicer and TRBP. In RLC, an ATP-dependent RNA helicase unwinds mature shRNA causing conformational changes that activate RISC, which separates the two strands (Nykänen *et al.* 2001;

Zhou *et al.* 2010; Hutvágner and Zamore 2002). Passenger strand is released whereas the single-stranded guide strand (antisense) will be used to identify the target mRNA, which is cleaved or conformationally changed and undergoes sequestration or degradation in processing bodies (p-bodies) containing mRNA degradation factors (Figure 6G). Each RLC is capable of executing multiple rounds of RNA interference (Yi *et al.* 2005; Rao *et al.* 2009b; Zhou *et al.* 2010).

Ago2 is the only member of the argonaute family with endonuclease activity capable of separating the strands of the shRNA. Nevertheless, the three remaining members of this family are also present in RLC, where they find complementary target sites in mRNAs so that Ago can initiate degradation, and they also bind target mRNA to block translation (Rao *et al.* 2009b; Hammond *et al.* 2001a).

The shRNA technique allows production of stable knockdown cell lines, with high reproducibility. Although it is a time-consuming technique, has high specificity and selectivity, is efficient and its effect is more durable once shRNA is continuously synthesized (Moore *et al.* 2010; Rao *et al.* 2009b).

2. Aims of the Dissertation

RNA interference approaches represent powerful strategies for unravelling putative gene functions in human cells. Since the function of novel PP1 complexes: BRI2:PP1 and BRI3:PP1 recently identified by our group remains poorly understood, we decided to induce the knockdown of PP1alpha and PP1gamma using the short-hairpin RNA interference strategy. Using this strategy, we will mimic the cellular behaviour in the absence of PP1alpha and PP1gamma and observe its effects on binding partners BRI2 and BRI3, particularly on expression levels of the later proteins.

Additionally, following both proteins *in vivo* using live cell imaging is a good strategy for further characterization of the complexes and additional functional assays. Therefore the production of fluorescent constructs for PP1alpha, PP1gamma1 and PP1gamma2 represents a mandatory task.

The specific aims of this dissertation are the following:

- To optimize human PP1alpha and PP1gamma shRNAs;
- To determine the effect of PP1alpha and PP1gamma knockdown on the expression and localization of BRI2 and BRI3;
- To generate PP1alpha, PP1gamma1 and PP1gamma2 fused GFP/DsRed-Monomer constructs.

3. Materials and Methods

3.1. shRNA Optimization

Human and rat PP1alpha and PP1gamma shRNA constructs were previously designed and produced in our laboratory, using RNAi-Ready pSiren-RetroQ, a self-inactivating retroviral expression vector with 6445bp designed to express an shRNA using the human U6 promoter (P_{U6}), RNA Polymerase III-dependent (*see Appendix*). This vector contains a puromycin resistance gene for selection of stable transfectants and an *E. coli* ampicillin resistance gene for propagation and selection in bacteria.

3.1.1. LB/Ampicillin Plates Preparation

Luria-Bertani (LB) medium plus agar plates containing ampicillin antibiotic were made. LB medium and agar were diluted in distilled water and autoclaved. After cooling to approximately 55°C, ampicillin was added at a concentration of 100 µg/mL. The medium was poured into plates that were left to cool and solidify.

3.1.2. *E. coli* XL1-Blue Transformation with shRNA vectors

For transformation of *E. coli* XL1-Blue, 5 ng of the shRNA plasmids for human and rat PP1alpha and PP1gamma were added to 50 µL of competent cells and gently mixed. The microtubes were incubated on ice for 20 minutes and heat shocked at 42°C for 70 seconds. After a 2 minutes incubation on ice, 450 µL of SOC medium were added to the microtubes, which were subsequently incubated at 37°C for 60 minutes with shaking at 180 rpm. The culture was then centrifuged at 14000 rpm for 1 minute and the supernatant was discarded. The cells were resuspended in the remaining supernatant (≈50 µL) and spread in the LB/agar medium plates containing ampicillin (100 µg/mL) previously prepared. The plates were incubated at 37°C overnight. Control transformations were also performed.

3.1.3. Isolation and Purification of the shRNAs

A single bacterial colony was transferred into 3 mL of LB medium containing ampicillin (100 µg/mL) and incubated overnight (12 to 16 hours) at 37°C with shaking at 180 rpm. The 3 mL

culture was used to inoculate 200 mL of LB medium with ampicillin (100 µg/mL) that grown overnight at 37°C with shaking at 180 rpm.

For DNA purification, *NucleoBond® Xtra Midi Kit* by *Macherey-Nagel* was used according to the manufacturer's protocol. The bacterial culture was poured into 50 mL tubes and centrifuged at 3200 xg for 15 minutes at 4°C. The supernatant was discarded and the pellet was resuspended in 8 mL of *Resuspension Buffer* with RNAse A. Then, 8 mL of *Lysis Buffer* were added to the cells and mixed gently by inverting the tube 5 times and left to incubate for 5 minutes. Next, 8 mL of the *Neutralization Buffer* were added to the suspension and immediately mixed by gently inverting the tubes 10 to 15 times. An additional centrifugation of 15 minutes at 12000 xg and at 4°C was added to separate the white flocculate from the homogeneous lysate. The lysate was then loaded onto the *NucleoBond® Xtra Column* with the *NucleoBond® Xtra Column Filter*, previously equilibrated with 12 mL of *Equilibration Buffer*, and was left to empty by gravity flow. After the loading, the column was washed with 5 mL of *Equilibration Buffer*. Then, the column filter was discarded and the column was washed with 8 mL of *Wash Buffer*. Finally, *Elution Buffer* was added to the column and the eluate was collected into a tube. To precipitate the DNA, 3.5 mL of room temperature isopropanol were added to the eluate, vortexed thoroughly and centrifuged at 15000 xg for 30 minutes at 4°C. The supernatant was discarded and 2 mL of room temperature 70% ethanol were added to the pellet and centrifuged at 15000 xg for 5 minutes. The ethanol was removed and the pellet was left to dry at room temperature. The DNA was reconstituted in 200 µL of sterile H_2O and the DNA concentration and 260/280 nm purity ratio was determined by absorbance measurements in NanoDrop 2000 UV-Vis Spectrophotometer.

3.1.4. Cell Culture

3.1.4.1. SH-SY5Y Culture

SH-SY5Y human neuroblastoma cells are derived from the cell line SK-N-SH (ATCC, Barcelona, Spain; CLR-2266), from a bone marrow biopsy of neuroblastoma patients. The cells were grown in complete SH-SY5Y medium: Minimal Essential Medium (MEM):F12 (1:1), supplemented with 10% Fetal Bovine Serum (FBS) with 2 mM L-glutamine, 100 U/mL penicillin and 100 mg/mL streptomycin. Cultures were maintained at 37°C and 5% CO_2. Cells were subcultured whenever approximately 90-95% confluency was reached.

3.1.4.2. Primary Neuronal Culture

Rat cortical cultures were established from Wistar Hannover 18 days rat embryos whose mother was euthanized by rapid cervical dislocation. After cortex dissection, tissues were dissociated with 0.23 mg/mL of trypsin and 0.15 mg/mL of deoxyribonuclease I in Hank's Balanced Salt Solution (HBSS) for 5 minutes at 37°C. Cells were washed with HBSS supplemented with 10% FBS to stop trypsinization, centrifuged at 1000 rpm for 2 minutes, and further washed and centrifuged with HBSS for serum withdrawal. Cells pellet was resuspended in complete Neurobasal medium from *Gibco®*, a serum-free medium combination, which is supplemented with 2% B-27 from *Gibco®*. The medium was also supplemented with glutamine (0.5 mM) and gentamicin (60 µg/mL). Viability and cellular concentration were assessed using the Trypan Blue excluding dye from *Sigma*. For immunoblotting analysis, cortical primary neuronal cultures were plated on poly-D-lysine-coated 6-well plates at a density of $0.8x10^6$ cells per well. Cells were maintained in 2 mL of Neurobasal medium in six-well plates in an atmosphere of 5% CO_2 at 37°C for 10 days before being used for experimental procedures. Five days after plating, ¼ of medium was replaced with complete Neurobasal medium.

3.1.5. Transfection

Human PP1alpha and PP1gamma shRNAs were transfected in SH-SY5Y neuroblastoma cells with both Lipofectamine and TurboFect (described below). shRNA for rat PP1alpha and PP1gamma was transfected in rat primary neuronal cultures only with Lipofectamine, since that is the recommended methodology for the transfection of primary cultures. In a preliminary study, 2 µg and 5 µg of DNA were transfected and subsequently the condition 3.5 µg of DNA was added to the study.

Approximately 24 hours before transfection, SH-SY5Y neuroblastoma cells were grown in 6-well plates at a density of $2.0x10^6$ of cells per plate with complete SH-SY5Y cell medium until 90% confluency was reached.

3.1.5.1. TurboFect

TurboFect™ Transfection Reagent from *Thermo Scientific* is a solution of a cationic polymer in water, which interacts with DNA forming positively charged, compact, stable and highly diffusible complexes that protect DNA from degradation and facilitate efficient plasmid delivery into eukaryotic cells. Following endocytosis of the DNA/TurboFect complexes, the reagent creates a proton-sponge effect that buffers endosomal pH by provoking massive proton accumulation and passive chloride influx. The endosome ruptures in the cytosol due to rapid osmotic swelling and DNA is translocated to the nucleus.

DNA was diluted in serum- and antibiotic/antimycotic (AA)-free SH medium. Then, TurboFect reagent (2 µL for each µg of DNA), previously vortexed, was added to the diluted DNA and mixed with the pipette. The solution was left at room temperature for 20 minutes to allow DNA-cationic polymer complexes formation. Meanwhile, the cells' medium was replaced by new SH complete medium. The complexes were added to the wells drop by drop and with gentle rocking of the plate. The cells were incubated at 37°C and 5% CO_2 for 6 hours at the end of which the medium was replaced by SH complete medium. The cells continued to incubate at the same conditions. Cells were harvested 24 and 48 hours after transfection. The medium was collected into microtubes and centrifuged for 5 minutes at 500 xg and at 4°C. The supernatant was discarded and 1 mL of 1x Phosphate Buffered Saline (PBS) was added to the tubes and centrifuged in the same conditions. The supernatant was discarded. Meanwhile, each well was washed with 1 mL of 1x PBS, which was then removed. To collect the cells, 200 µL of boiled 1% Sodium Dodecyl Sulphate (SDS) was added to each well and transferred to the pellet obtained previously. Finally, the samples were boiled for 10 minutes at 90°C and sonicated for 10 seconds.

3.1.5.2. Lipofectamine

Lipofectamine 2000™ Transfection Reagent from *Invitrogen™* is a cationic liposome, which forms a complex with negatively charged DNA molecules to overcome the electrostatic repulsion of the cell membrane. The complex liposome/nucleic acid is believed to enter into the cell through endocytosis.

DNA was diluted in serum- and AA-free Dulbecco's Modified Eagle's Medium (DMEM) and *Lipofectamine 2000 reagent* (4 µL of Lipofectamine for each µg of DNA) was diluted in the same

medium. The tubes were incubated for 5 minutes at room temperature. Then, the DNA was added to the Lipofectamine solution drop by drop and gently mixed with the micropipette. In order to form the DNA-lipid complexes, the tubes were allowed to rest for 20 minutes at room temperature. Meanwhile, the cells' medium was replaced by serum- and AA-free medium. The complexes were added and the cells were incubated and harvested as described above for transfection with TurboFect reagent.

3.1.6. Resazurin Cell Viability Assay

Resazurin assay is a colorimetric assay that detects cellular metabolic activity and offers a sensitive measurement for the viability of cells. Resazurin is a blue nonfluorescent dye that is reduced into the pink coloured and strongly fluorescent dye resorufin by dehydrogenase enzymes present in metabolically active cells. Once this conversion only occurs in viable cells, the amount of resorufin produced is proportional to the number of viable cells in the sample and can be quantified by measuring the relative fluorescent units.

4 hours before each harvest (24 and 48 hours), 10% of resazurin/ 1x PBS solution was added to each well and the plates were shaken and incubated at 37°C and 5% CO_2. Absorbance was measured at 570 nm and 600 nm, using the *Infinite M200 Tecan* and *I-control™* software.

3.1.7. BCA Protein Assay

Measurements of total protein concentration were carried out using *Pierce's BCA Protein Assay Kit*, according to the manufacturer's instructions. This procedure is based on the reduction of Cu^{2+} to Cu^{+} by protein in an alkaline medium and the highly sensitive and selective colorimetric detection of the cuprous cation (Cu^{+}) by bicinchoninic acid (BCA). The chelation of two molecules of BCA with one cuprous ion results in the formation of a purple-coloured reaction product. This water-soluble complex exhibits a strong linear absorbance at 562 nm with increasing protein concentrations.

This procedure was carried out in a 96-well plate and the protein standards were prepared with Bovine Serum Albumin (BSA) as described in Table 1. The samples were prepared by diluting 5 µL

of each sample in 20 µL of 1% SDS. Duplicates of both standards and samples were always prepared.

Table 1 BSA Standards used in the BCA Protein Assay. *BSA, bovine serum albumin; SDS, sodium dodecyl sulphate; WR, working reagent.*

Standard	BSA (µL)	1% SDS (µL)	Protein Mass (µg)	WR (µL)
P0	---	25	0	200
P1	1	24	2	200
P2	2	23	4	200
P3	5	20	10	200
P4	10	15	20	200
P5	20	5	40	200

The Working Reagent (WR) was prepared by mixing BCA Reagent A with BCA Reagent B in the proportion 50:1. Then, 200 µL of WR were added to each sample. The plate was incubated at 37°C for 30 minutes. The plate was left to cool at room temperature and then the absorbance was measured at 562 nm, using the *Infinite M200 Tecan* and *I-control™* software.

A standard curve was obtained by plotting BSA standard absorbance vs BSA concentrations and was used to determine the total protein concentration of the samples.

3.1.8. SDS-PAGE

After BCA quantification, proteins were separated by SDS-Polyacrylamide Gel Electrophoresis (SDS-PAGE), according to their molecular weight. To visualize PP1alpha and PP1gamma, with 37 kDa, a 12% polyacrylamide running gel was prepared. The running and stacking gels were prepared as described in Table 2**.**

Table 2 Components of the running and stacking gels for SDS-PAGE. *APS, ammonium persulfate; LGB, lower gel buffer; SDS, sodium dodecyl sulphate; TEMED, N, N, N', N'-Tetramethylethylenediamine; UGB, upper gel buffer.*

Components	Running Gel (12%)	Stacking Gel (3.5%)
Water	20.7 mL	13.2 mL
30% Acryl/8% Bisacryl	24 mL	2.4 mL
4x LGB	15 mL	---
5xUGB	---	4 mL
10% SDS	---	200 µL
10% APS	300 µL	200 µL
TEMED	30 µL	20 µL

The samples were prepared by the addition of ¼ volume of loading gel buffer (LB) and boiled at 90°C for 3-5 minutes. The protein marker used was *Precision Plus Protein™ Dual Color Standards* from *Bio-Rad*. The gel ran at 90 mA for approximately 4 hours.

3.1.9. Immunoblotting

The proteins in the polyacrylamide gel were transferred to a nitrocellulose membrane from *GE Healthcare Life Sciences* at 200 mA, during approximately 18 hours. To assess gel loading, Ponceau S solution was applied to the nitrocellulose membrane. Ponceau S is a negative stain that binds to positively charged amino groups of proteins and also binds non-covalently to non-polar regions in the protein. It is a rapid, nontoxic and reversible staining method that generates reddish pink protein bands and allows further immunological detection. The nitrocellulose membranes were incubated for 7 minutes at room temperature and rinsed with distilled water. The result was scanned in *GS-800 Calibrated Densitometer* and quantified through the *1-D Analysis Quantity One* and *ImageLab™* software from *Bio-Rad*. Membranes were washed in 1x Tris Buffered Saline + Tween (TBST) with gentle agitation until the staining was completely eliminated.

3.1.9.1. Membrane incubation

The membranes were hydrated in 1x TBS for 5 minutes and incubated with a 5% non-fat dry milk/1x TBST solution for blocking the non-specific binding sites, during approximately 4 hours with shaking. The membranes were incubated with the primary antibodies Rabbit Polyclonal CBC2C (1:2500) and CBC3C (1:5000) (Cruz e Silva *et al.* 1995) that recognize the C-terminal of

PP1alpha and PP1gamma, respectively, diluted in 3% non-fat dry milk/1x TBST with shaking for 4 hours at room temperature and overnight at 4°C. After washed 3x 10 minutes with 1x TBST, the membranes were incubated with an Anti-Rabbit Horseradish Peroxidase (HRP) conjugated secondary antibody (1:5000) diluted in 3% non-fat dry milk/1x TBST with shaking for 2 hours at room temperature. A final 3x 10 minutes wash with 1x TBST was performed before the detection.

Membranes were reused to incubate with primary antibodies for BRI2 and BRI3, after being stripped with stripping solution for 30 minutes at 50°C and washed with 1x TBST. The blocking solutions used in membranes that incubated with BRI2 and BRI3 antibodies were 5% BSA/1x TBST and 5% non-fat dry milk/1x TBST, respectively. The primary antibodies Mouse Monoclonal BRI2 C-8 (1:500) from *Santa Cruz Biotechnology, Inc.*, that recognizes the N-terminal of BRI2, diluted in 3% BSA/1xTBST, and Rabbit Polyclonal BRI3 (1:750) from *Abcam*, raised against amino acids 110-258 of human BRI3, diluted in 3% non-fat dry milk/1x TBST, incubated overnight at 4°C. The Anti-Rabbit and Anti-Mouse Horseradish Peroxidase (HRP) conjugated secondary antibodies (1:5000), diluted in 3% non-fat dry milk/1x TBST, incubated for 2 hours. 1x TBST washes were performed as previously described.

3.1.9.2. Immunodetection

Immunodetection was performed using *Luminata™ Crescendo Western HRP Substrate* from *Millipore*, a chemiluminescent non-radioactive method for detection of specific antigens, conjugated directly or indirectly with HRP-labelled antibodies. The membranes were incubated with *Luminata™ Crescendo* for 2 to 5 minutes at room temperature and then, X-ray films from *Kodak* were exposed, developed and fixed with appropriate solutions. The X-rays films were scanned in *GS-800 Calibrated Densitometer* and quantified through the *1-D Analysis Quantity One* and *ImageLab™* software from *Bio-Rad*.

3.2. Effects of human PP1alpha and PP1gamma knockdown on Expression and Processing of BRI2 and BRI3

After human PP1alpha and PP1gamma shRNA optimization, transfection was repeated with the best conditions: 48 hours transfection of 3.5 µg using TurboFect reagent (sections 3.1.5 and 3.1.5.1). Total protein concentration was measured by BCA Protein Assay followed by SDS-PAGE,

as described in sections 3.1.7 and 3.1.8, respectively. Immunoblotting was performed as described in section 3.1.9 to assess PP1alpha and PP1gamma expression and also BRI2 and BRI3 expression.

3.3. PP1 Fluorescent Constructs

In our laboratory we have PP1alpha, PP1gamma1 and PP1gamma2 in pAS2-1 vectors and we wanted to insert these PP1 isoforms in fluorescent vectors, pAcGFP1-C1 and pDsRed-Monomer-C1, using the restriction enzymes (RE) *EcoRI* and *BamHI*. Thus, we used Polymerase Chain Reaction (PCR) Subcloning. PCR Subcloning procedure includes amplification of the interest fragment by PCR, purification of the PCR products, ligation of the gene to the new vector and finally transformation of the ligation in bacteria.

pAS2-1 is a yeast two-hybrid expression vector with 8393bp. It contains an *E. coli* ampicillin resistance gene and in the multiple cloning site (MCS), restrictions sites for RE *EcoRI* and *BamHI* (*see Appendix*).

pAcGFP1-C1 and pDsRed-Monomer-C1 are mammalian expression vectors both with 4700bp. pAcGFP1-C1 (*see Appendix*) encodes a green fluorescent protein (GFP) from *Aequorea coerulescens*, that when expressed in cells, generates green fluorescence detectable by fluorescent microscopy. The vector contains an *E. coli* kanamycin resistance gene and restriction sites for the RE *EcoRI* and *BamHI* in the MCS. pDsRed-Monomer-C1 (*see Appendix*) encodes DsRed-Monomer (DsRed.M1), a monomeric mutant derived from the tetrameric *Discosoma sp.* red fluorescent protein, with forty-five amino acid substitutions. 12-16 hours after transfection of the vector in mammalian cells and expression of the protein, red-emitting cells can be detected by fluorescent microscopy or flow cytometry. As pAcGFP1-C1 vector, pDsRed-Monomer-C1 has an *E. coli* kanamycin resistance gene and restrictions site for *EcoRI* and *BamHI* in the MCS.

3.3.1. *E. coli* XL1-Blue Transformation with pAS2-1 vectors

E. coli XL1-Blue transformation with the pAS2-1 plasmids containing PP1alpha, PP1gamma1 and PP1gamma2 was performed as described in section 3.1.2. 5 ng of each vector were added to 50 µL of competent cells and the resuspended bacterial cells were spread in LB/agar plates

previously prepared as described in section 3.1.1, but containing, instead of ampicillin, kanamycin at a concentration of 30 µg/mL.

3.3.2. Isolation and Purification of the pAS2-1 vectors

A single bacterial colony of each plate was inoculated into a test-tube with 3 mL of LB medium containing kanamycin (30 µg/mL) and incubated overnight at 37°C with shaking at 180 rpm. For DNA purification, *QIAprep Spin Miniprep Kit* from *QIAGEN®* was used according to the manufacturer's instructions. 1.5 mL of each culture was poured into a microtube and centrifuged at 8000 rpm for 3 minutes at room temperature. The bacterial pellet was resuspended in 250 µL of *Buffer P1* with RNAse A. To lyse the bacterial cells, 250 µL of *Buffer P2* were added and gently mixed by inverting the tube 4 to 6 times until the solution becomes viscous. Then, 350 µL of neutralizer *Buffer N3* were added and immediately and thoroughly mixed by inverting the tube 4 to 6 times, obtaining a cloudy solution, which was centrifuged at 13000 rpm for 10 minutes. The supernatants were applied to the *QIAprep Spin Column* by pipetting and centrifuged at 14000 rpm for 1 minute. The columns were washed with 500 µL of *Buffer PB*, in an additional step, and centrifuged again at 14000 rpm for 1 minute. 750 µL of *Buffer PE* were added to wash the columns, which were centrifuged once more at 14000 rpm for 1 minute. Lastly, an additional 1 minute centrifugation at 14000 rpm was performed to remove residual wash buffer. The flow-throughs were always discarded. The *QIAprep Column* was placed in a clean 1.5 mL microtube and the DNA was eluted in 50 µL of sterile H_2O. After adding the water to the centre of each column, it was left to incubate for 1 minute and then centrifuged at 14000 rpm for 1 minute. The DNA concentration and 260/280 nm purity ratio was determined by absorbance measurements in NanoDrop 2000 UV-Vis Spectrophotometer.

3.3.3. Polymerase Chain Reaction Amplification

Sense and Antisense primers were designed for each PP1 isoform coding sequence. *EcoRI* and *BamHI* restriction sites were inserted in the forward and reverse primers, respectively. The primers' sequences and melting temperatures (MT) are indicated in appendix III.

Polymerase Chain Reaction (PCR) was performed to amplify the PP1alpha, PP1gamma1 and PP1gamma2 coding sequences with enzymes restriction sites. The reaction components indicated

below were mixed in 0.2 mL PCR microtubes and the cycling conditions used are described in Table 3.

Reaction setup:

- 10x Buffer for KOD Hot Start DNA Polymerase 5 µL
- 25 mM $MgSO_4$ 3 µL
- dNTP's 5 µL
- PCR Grade Water 31 µL
- Sense Primer (10 µM) 1.5 µL
- Antisense Primer (10 µM) 1.5 µL
- 100 ng Template DNA 2 µL
- KOD Hot Start Polymerase (1 U/µL) 1 µL
- Total Reaction Volume 50 µL

Table 3 PCR cycling conditions.

Step	Temperature	Time	Cycles
Hot Start	95°C	---	---
Polymerase Activation	95°C	2 minutes	1
Denature	95°C	20 seconds	25
Annealing	56°C	10 seconds	
Extension	70°C	15 seconds	
Hold	4°C	∞	---

3.3.4. Agarose Gel Electrophoresis

After PCR, a 1% agarose gel was made. The required amount of agarose was weighted and dissolved in 1x TAE buffer. The agarose was heated until dissolved and homogenized. The electrophoresis apparatus from *Bio-Rad* was prepared and the comb was correctly placed. The agarose solution was allowed to cool to 60°C and *GreenSafe Premium* (3 µL of greensafe to 100 mL of solution) from *NZYTech*, was added and gently mixed. The gel was poured into the gel tray until polymerization. The samples of the PCR products were prepared with 6x Loading Buffer (LB). Sterile water was added to make up the appropriate volume, when required. The gel was placed in the electrophoresis tank, covered with 1x TAE and the comb was removed carefully. The molecular marker (MM) *1 Kb Plus DNA Ladder* from *Invitrogen™* and the samples were loaded

into the gel, which ran at 90 volts for approximately 1 hour. The gel was analyzed and photographed using *Gel Doc™ XR+ System* and *ImageLab™* software from *Bio-Rad*.

3.3.5. Enzyme Restriction

A restriction of the PCR products and the vectors GFP-C1 and DsRed-Monomer-C1 containing BRI2, was performed using restriction endonucleases *EcoRI* and *BamHI* from *New England Biolabs*. Compatibility between the two enzymes was confirmed and a double digestion was carried out using 100x BSA and 10x NEBuffer *EcoRI*. For the vectors restriction, 0.75 µL of *EcoRI* and 1.5 µL of *BamHI* were used. In the case of the inserts, it was used 1 µL of *EcoRI* and 1.5 µL of *BamHI*. Sterile water was added to make up the total volume, 20 µL and 60 µL for the vectors and inserts, respectively. The reactions were incubated at 37°C overnight and heat inactivation was performed at 65°C for 20 minutes. To confirm the enzyme restriction, a 0.8% agarose gel was made as described in section 3.3.4, using 3 µL of the reaction to prepare the samples.

3.3.6. DNA Extraction

After the restriction, 6x LB was added to the samples, which ran in a 0.8% agarose gel (section 3.3.4) for DNA extraction. The extraction was carried out using *NucleoSpin® Gel and PCR Clean-up Kit* by *Macherey-Nagel*, according to the manufacturer's instructions. The DNA fragments were excised from the agarose gel, put in 2 mL microtubes and weighted. For each 100 mg of agarose gel, 200 µL of *Buffer NTI* was added. The samples were incubated at 50°C for 10 minutes and vortexed every 2-3 minutes until the gel slice was completely dissolved. Then, the samples were loaded (700 µL at a time) into the *NucleoSpin® Gel and PCR Clean-up Column* placed in a Collection Tube (2 mL) and centrifuged for 30 seconds at 11000 xg. The silica membranes were washed two times with 700 µL of Buffer NT3 and centrifuged for 30 seconds at 11000 xg. Subsequently, a 3 minute centrifugation at 11000 xg was done to dry the silica membrane and remove *Buffer NT3* completely. The flow-throughs were always discarded. The columns were placed into new 1.5 mL microtubes and 30 µL (15 µL at a time) of *Buffer NE* were added, incubated for 2 minutes at room temperature and centrifuged for 1 minute at 11000 xg.

A 0.8% agarose gel (section 3.3.4) was made to determine the concentration of the extracted DNA using the quantity tools of the *ImageLab™* software from *Bio-Rad* and *1 Kb Plus DNA Ladder* from

Invitrogen™ as reference (when 5 µL are loaded, the 1650bp band has 40 ng of DNA). Additionally, the DNA concentration and 260/280 nm purity ration were determined by absorbance measurements in NanoDrop 2000 UV-Vis Spectrophotometer.

3.3.7. Vector Dephosphorylation

To prevent vector recircularization, dephosphorylation of the 5' ends of GFP-C1 and DsRed-Monomer-C1 vectors was performed, using *Alkaline Phosphatase* from *NZYTech*, according to the manufacturers' instructions. For a total volume of 25 µL, 20 µL of each vector were mixed with 2.5 µL of 10x Reaction Buffer, 2 µL of alkaline phosphatase (0.5 U/µL) and 0.5 µL of sterile water. The reaction was incubated at 37°C for 1 hour and then inactivated for 10 minutes at 65°C.

3.3.8. Ligation

The ligation between the extracted and dephosphorylated vectors and the extracted inserts was executed using T4 DNA Ligase from *New England BioLabs*. Six ligations were made between each one of the inserts, PP1alpha, PP1gamma1 and PP1gamma2, and both vectors, GFP-C1 and DsRed-Monomer-C1. Controls containing only vector and no insert were also prepared. 50 ng of vector were used in the ligation reactions. The vector:insert ratios used were 1:3 and 1:6 and the amount of insert needed was calculated by the formula $\frac{50ng \times Kb_{insert}}{Kb_{vector}} \times \frac{3}{1}\ ng$ and $\frac{50ng \times Kb_{insert}}{Kb_{vector}} \times \frac{6}{1}\ ng$, respectively. Besides the vector and insert, the ligation reactions contained 10x T4 DNA Ligase Buffer, 1 µL of T4 DNA Ligase and sterile water to make up the total volume of 20 µL. The reactions were incubated overnight at 16°C and heat inactivated at 65°C for 10 minutes.

3.3.9. *E. coli* XL1-Blue Transformation of Ligations

E. coli XL1-Blue transformation with the ligations was performed with 5 µL of each ligation and 100 µL of competent cells, as described in section 3.1.2. However, some alterations were made: the bacterial cells were heat shock at 42°C for 90 seconds; 900 µL of SOC medium were added to the microtubes, which were incubated at 37°C for 2 hours and 30 minutes; and the resuspended

bacterial cells were spread in LB/agar plates previously prepared as described in section 3.1.1, but containing, instead of ampicillin, kanamycin at a concentration of 30 µg/mL.

3.3.10. Plasmid DNA Extraction - Alkaline Lysis Method

The colonies that grew in the ligation plates were transferred into 3 mL of LB medium containing kanamycin (30 µg/mL) and incubated overnight at 37°C with shaking at 180 rpm.

To extract the plasmid DNA from the bacterial cells, alkaline lysis method was performed. First, 1.5 mL of the bacterial cultures were poured into microtubes and centrifuged for 1 minute at 12000 xg and 4°C. The supernatant was discarded. The pellet was resuspended in 100 µL of Solution I (*see appendix*) and vigorously vortexed. To lyse the cells, 200 µL of Solution II (*see appendix*) were added and mixed by inverting the tube five times, obtaining a viscous bacterial lysate. The microtubes were stored on ice. Then, 150 µL of Solution III (*see appendix*) were added and gently vortexed for 10 seconds in an inverted position. The microtubes were stored on ice for 3 to 5 minutes. Finally, a 10 minute centrifugation was performed at 12000 xg and 4°C and the clear supernatant was transferred to a new microtube. To precipitate the DNA, 2 volumes of 100% ethanol (900 µL) at room temperature were added and mixed by vortexing. The solutions were left to stand 30 minutes at −20°C and then centrifuged for 10 minutes at 14000 xg and 4°C. The supernatant was discarded and 1 mL of 70% ethanol were added to the microtubes. After 5 minutes at −20°C, a centrifugation of 5 minutes at 12000 xg and 4°C was performed. The supernatant was discarded and the DNA pellet was allowed to dry completely and then redissolved in 50 µL of H_2O containing RNAse (20 µg/mL), briefly vortexed and stored at −20°C.

3.3.11. DNA Restriction and Electrophoretic Analysis

To confirm the presence of positive clones, a sample of DNA of each ligation was cut with the same restriction endonucleases used in section 3.3.5, *EcoRI* and *BamHI*, and run in an agarose gel.

A restriction mix was prepared with 100x BSA, 10x NEBuffer *EcoRI*, 2 µL of *EcoRI*, 3 µL of *BamHI* and sterile water to make up the required volume. The reactions contained 7 µL DNA and 7 µL mix, were incubated overnight at 37°C and heat inactivated at 65°C for 20 minutes.

After the addition of 6x LB to the restriction reactions, the samples were ready to be loaded and run in a 1% agarose gel, as described in section 3.3.4, to verify if the vector:insert ligation occurred.

4. Results

4.1. shRNA Optimization

Since the function of novel PP1 complexes (PP1:BRI2 and PP1:BRI3) recently identified by our group (Martins et al. 2014, submitted) remains poorly understood, we decided to use short hairpin RNA interference strategy to interfere *in vivo* with PP1alpha and PP1gamma and determine the effects on the binding patterns: BRI2 and BRI3. Therefore, we used specific PP1alpha and PP1gamma shRNA constructs to downregulate PP1alpha and PP1gamma, respectively. Both human and rat PP1alpha and PP1gamma shRNA constructs were previously generated in the laboratory and were tested and the transfection optimized.

4.1.1. shRNA for human PP1alpha and PP1gamma

In a preliminary study to optimize the human PP1alpha and PP1gamma shRNAs, we tested two different transfection reagents, two different DNA concentrations and also two different periods of transfection. The transfection conditions were optimized to establish the best RNA interference efficiency. Briefly, human PP1alpha and PP1gamma shRNA constructs were transfected in human SH-SY5Y neuroblastoma cells using both TurboFect and Lipofectamine transfection reagents. Two different amounts of DNA (2 µg and 5 µg) were transfected and the cells were harvested 24 and 48 hours after transfection. The same amounts of missense controls (MSC) were also transfected. The effect of shRNA transfection on the expression of both human PP1alpha and PP1gamma was monitored by SDS-PAGE, followed by immunoblotting using specific antibodies against PP1alpha and PP1gamma. PP1 isoform expression was always compared between cells transfected with shRNA missense control and cells transfected with human PP1alpha and PP1gamma specific shRNAs. Human PP1alpha and PP1gamma levels were quantified by densitometry and normalized with the loading control (Ponceau S). The results are presented in Figure 7. For PP1alpha, 24 hours upon transfection, an interference of approximately 25% and 45% was achieved using 2 µg and 5 µg of the construct, respectively. 48 hours post-transfection, no significant knockdown was observed. For PP1gamma, the knockdown efficiency was higher for both time periods (24 and 48 hours). The interference achieved was around 45% with 2 µg and 60% with 5 µg for 24 hours and the highest interference was achieved with 5 µg for 48 hours, around 80%.

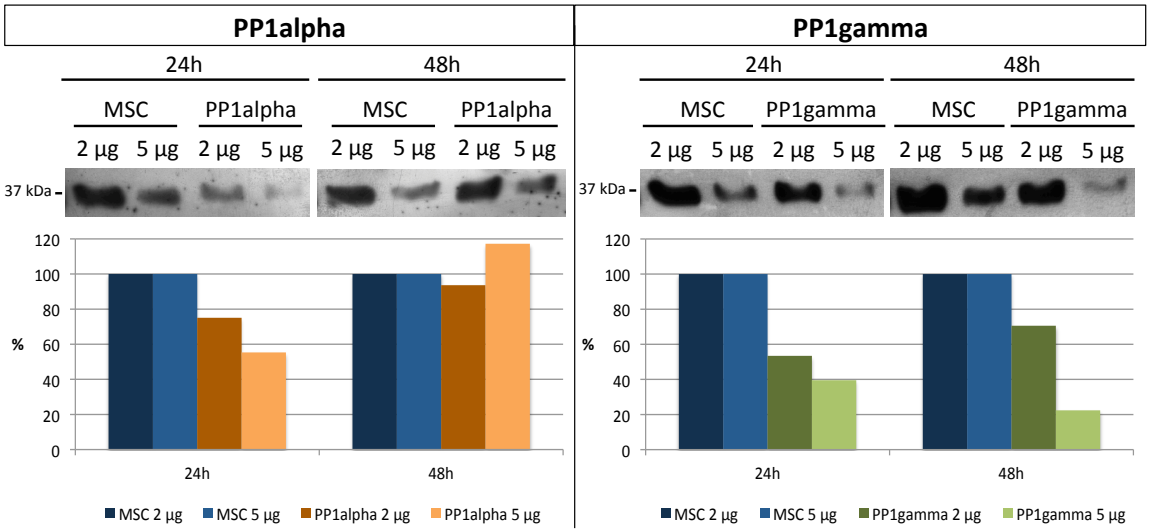

Figure 7 Knockdown levels of human PP1alpha (on the left) and PP1gamma (on the right), 24 and 48 hours upon transfection with TurboFect reagent, using 2 µg and 5 µg of each shRNA construct. *MSC, missense control.*

The results using the Lipofectamine transfection reagent are presented in Figure 8. The effects of knockdown after Lipofectamine transfection of SH-S5Y5 cells using both PP1 shRNAs were not so clear as those observed for transfection using TurboFect. In fact, no significant knockdown was observed 24 hours upon transfection, neither for PP1alpha nor PP1gamma. However, 40% interference was observed for PP1alpha with 2 µg at 48 hours but only 10% interference was achieved with 5 µg. The maximum interference with Lipofectamine was obtained for PP1gamma at 48 hours, achieving 60% and 80% knockdown with 2 µg and 5 µg, respectively.

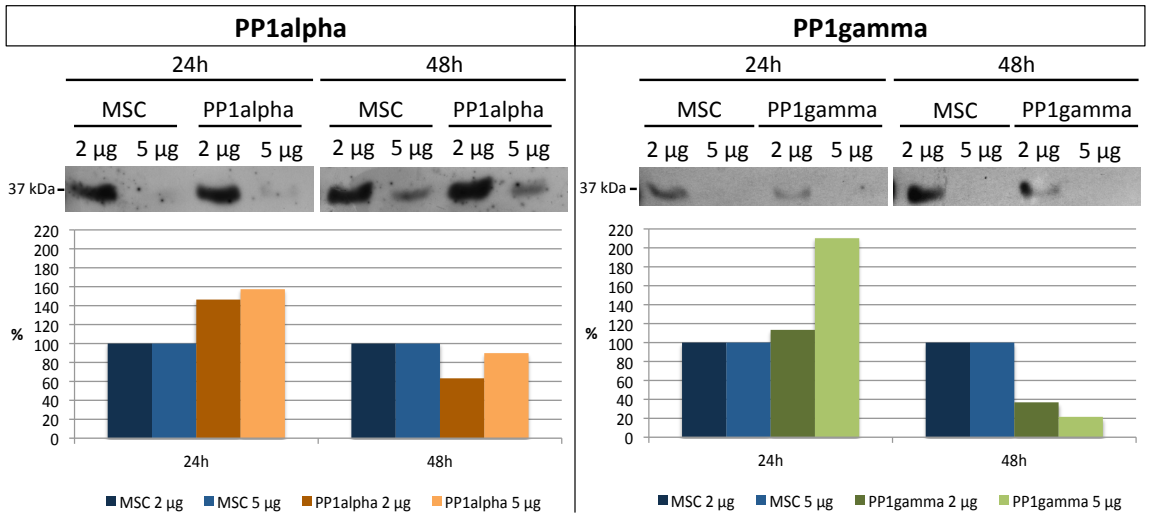

Figure 8 Knockdown levels of human PP1alpha (on the left) and PP1gamma (on the right), 24 and 48 hours upon transfection with Lipofectamine reagent, using 2 µg and 5 µg of each shRNA construct. *MSC, missense control.*

After analysis of the results of this preliminary study, it was concluded that TurboFect transfection reagent was more suitable for transfection of the PP1 shRNA constructs in SH-S5Y5 cells. Moreover, a new condition was added to the optimization study, 3.5 µg of DNA. The periods of transfection incubation, 24 and 48 hours, were maintained. Three DNA concentrations were now tested (2 µg, 3.5 µg and 5 µg) for 24 and 48 hours. The results are presented in Figure 9. For PP1alpha (left panel), at 24 hours upon transfection of 2 µg of the shRNA construct, the interference achieved was approximately 15%. Transfection of 3.5 µg and 5 µg of the construct improved knockdown to approximately 30%. The interference observed at 48 hours for PP1alpha was around 35% for 2 µg and 5 µg and approximately 50% for 3.5 µg. For PP1gamma (right panel), only 10% and 20% interference was observed upon 24 hours and 48 hours of transfection with 2 µg of DNA. At 24 hours, using 3.5 µg and 5 µg of shRNA constructs, the interference on PP1gamma expression was approximately 30% and 20%, respectively. At 48 hours, with these DNA concentrations, the greatest knockdown of this PP1 isoform, approximately 50%, was obtained.

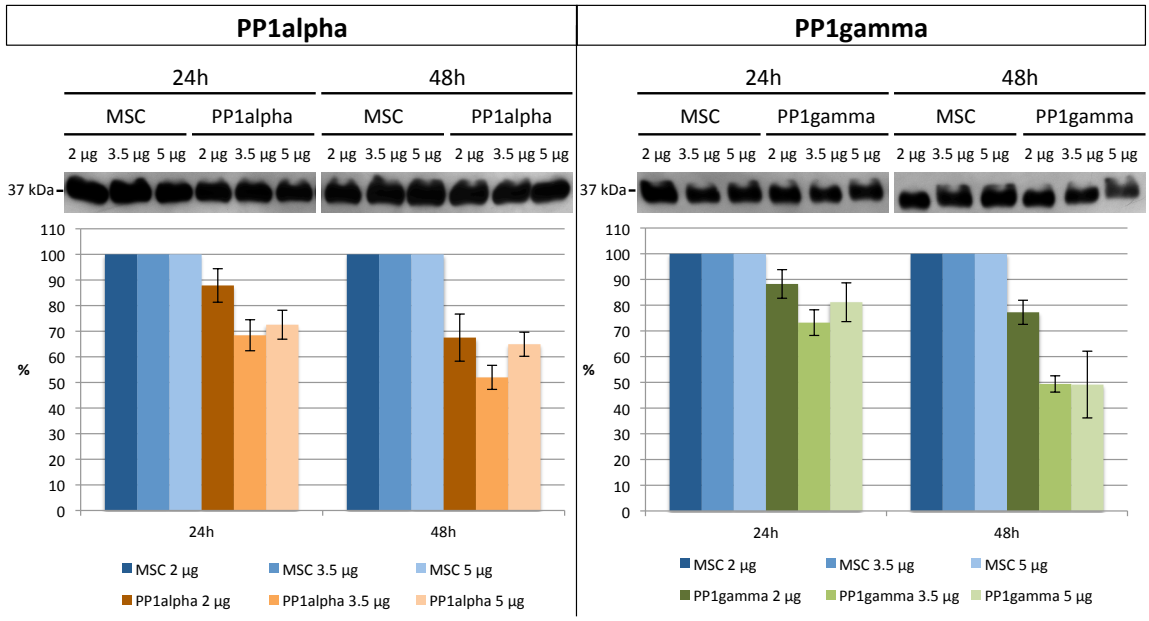

Figure 9 Knockdown levels of human PP1alpha (on the left) and PP1gamma (on the right), 24 and 48 hours upon transfection with TurboFect reagent, using 2 µg, 3.5 µg and 5 µg of each shRNA construct. Data are presented as mean ± Standard Error of the Mean (SEM) of four independent experiments (n=4). *MSC, missense control.*

4.1.1.1. Resazurin Viability Assay

Simultaneously we also determined cell viability of the SH-SY5Y cells TurboFect transfected with the three amounts of DNA (2 µg, 3.5 µg and 5 µg) for 24 hours and 48 hours. For that, we used a well characterized viability assay, named Resazurin assay. Briefly, SH-S5Y5 cells were transfected with three different amounts of shRNA constructs (missense controls, human PP1alpha and PP1gamma) using TurboFect reagent. Four hours before being harvested they were incubated with medium + resazurin and the absorbance at 570 nm and 600 nm was measured and compared with the non-transfected control (NTC). The results obtained are represented in Figure 10. In general, cell viability decreases with time and higher amounts of transfected DNA. Maximum decrease in cell viability was around 20% and 40% for PP1alpha and PP1gamma shRNA constructs, respectively. Transfection of the missense control also caused reduction of cell viability in 20%.

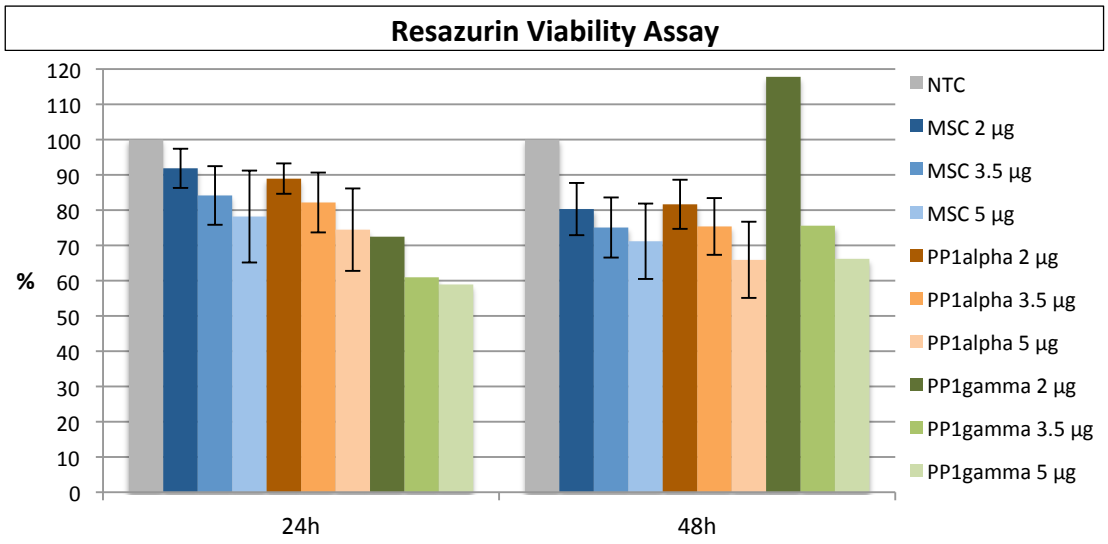

Figure 10 Resazurin viability assay. Resazurin assay to determine viability of SH-S5Y5 cells harvested 24 and 48 hours upon transfection of 2 µg, 3.5 µg and 5 µg of human PP1alpha, PP1gamma and missense control shRNA constructs with TurboFect reagent, compared with non-transfected cells. Data are presented as mean ± SEM of four independent experiments (n=4) for PP1alpha and two (n=2) for PP1gamma. *NTC, non-transfected control; MSC, missense control.*

4.1.2. shRNA for rat PP1alpha and PP1gamma

In a preliminary study, rat PP1alpha and PP1gamma shRNAs were transfected in rat cortical neurons using Lipofectamine transfection reagent. In this study, 2 µg and 5 µg of DNA were transfected and the cells were harvested 24 and 48 hours upon transfection. The same amounts of missense controls were also transfected. The effect of transfection of the shRNAs constructs on

the expression of both rat PP1alpha and PP1gamma was monitored by SDS-PAGE, followed by immunoblotting using specific antibodies against rat PP1alpha and PP1gamma. PP1 isoform expression was compared between cells transfected with shRNA missense control and cells transfected with rat PP1alpha and PP1gamma specific shRNAs. Rat PP1alpha and PP1gamma levels were quantified by densitometry and normalized with the loading control (Ponceau S). The knockdown levels of rat PP1alpha (left) and PP1gamma (right) 24 and 48 hours upon transfection are presented in Figure 11. No significant interference in rat PP1 levels was observed, except for PP1alpha 24 hours upon transfection where we observed approximately 40% of knockdown, using both DNA concentrations, and 20% knockdown for PP1gamma, 48 hours upon transfection with 5 µg of DNA.

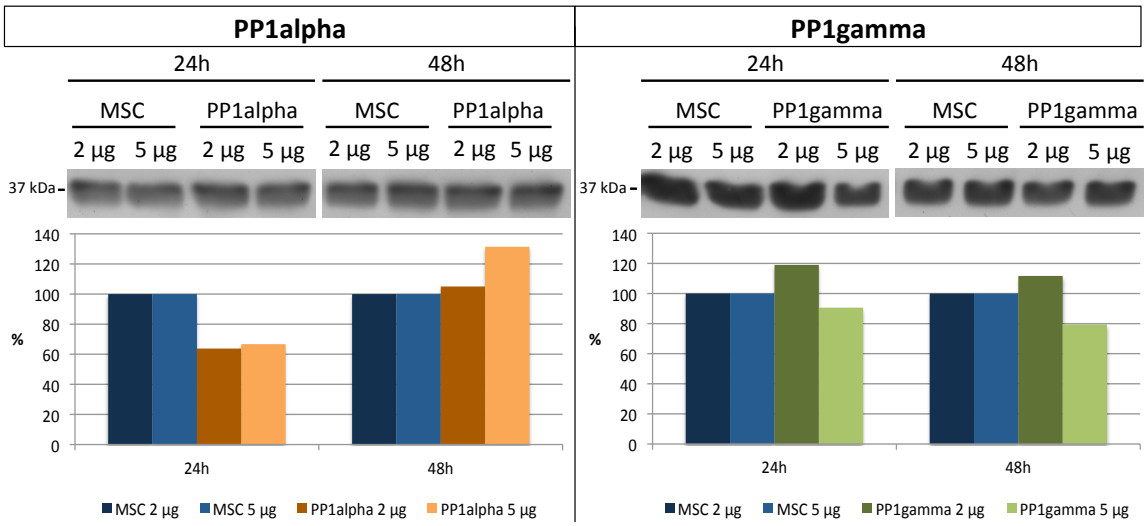

Figure 11 Knockdown levels of rat PP1alpha (on the left) and PP1gamma (on the right), 24 and 48 hours upon transfection with Lipofectamine reagent, using 2 µg and 5 µg of each shRNA construct. *MSC, missense control.*

4.2. Effect of human PP1alpha and PP1gamma Knockdown on the Expression and Processing of BRI2 and BRI3

After transfection optimization of human PP1alpha and PP1gamma shRNA constructs, the best transfection conditions selected were 48 hours transfection, 3.5 µg of each shRNA construct and using TurboFect. These conditions were used to transfect SH-SY5Y cells, in order to determine the effects of human PP1alpha and PP1gamma knockdown on BRI2 and BRI3 expression, through SDS-PAGE and immunoblotting using specific antibodies against PP1alpha, PP1gamma, BRI2 and BRI3 proteins. Protein levels were quantified by densitometry and normalized with the loading

control (Ponceau S). Human PP1alpha and PP1gamma knockdown was determined to confirm shRNA interference and the results are presented in Figure 12. Human PP1alpha and PP1gamma shRNA constructs produced approximately 20% and 35% knockdown, respectively.

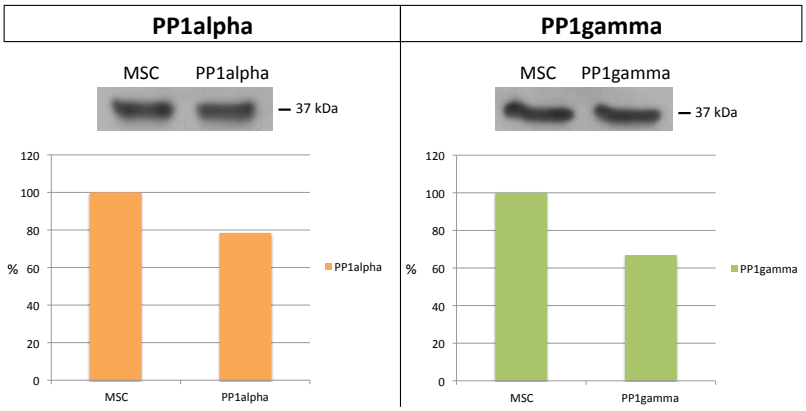

Figure 12 Knockdown levels of human PP1alpha (on the left) and PP1gamma (on the right), 48 hours upon transfection with TurboFect reagent, using 3.5 µg of each shRNA construct. *MSC, missense control.*

BRI2 and BRI3 expression was always compared between cells transfected with shRNA missense control and cells transfected with human PP1alpha and PP1gamma specific shRNAs. The results are presented in Figure 13. For both BRI2 (left panel) and BRI3 (right panel), two bands with a 3 kDa difference can be identified (detected slightly above and around 37 kDa for BRI2 and BRI3, respectively), which were quantified together (Figure 13A and B) and separately (Figure 13C and D). Total BRI2 expression levels decrease approximately 20% and 15% when we interfere with human PP1alpha and PP1gamma, respectively. After quantification of both BRI2 bands separately, we observed an increase of 30% and 20% of processed BRI2 expression levels with knockdown of human PP1alpha and PP1gamma, respectively. No differences were observed in the levels of unprocessed BRI2. The 20% knockdown of human PP1alpha caused a 20% increase in total BRI3 levels and 40% and 20% increase in unprocessed and processed BRI3, respectively. The 35% knockdown of human PP1gamma had no influence in total BRI3 expression. However, an increase of approximately 30% was observed in unprocessed BRI3 levels.

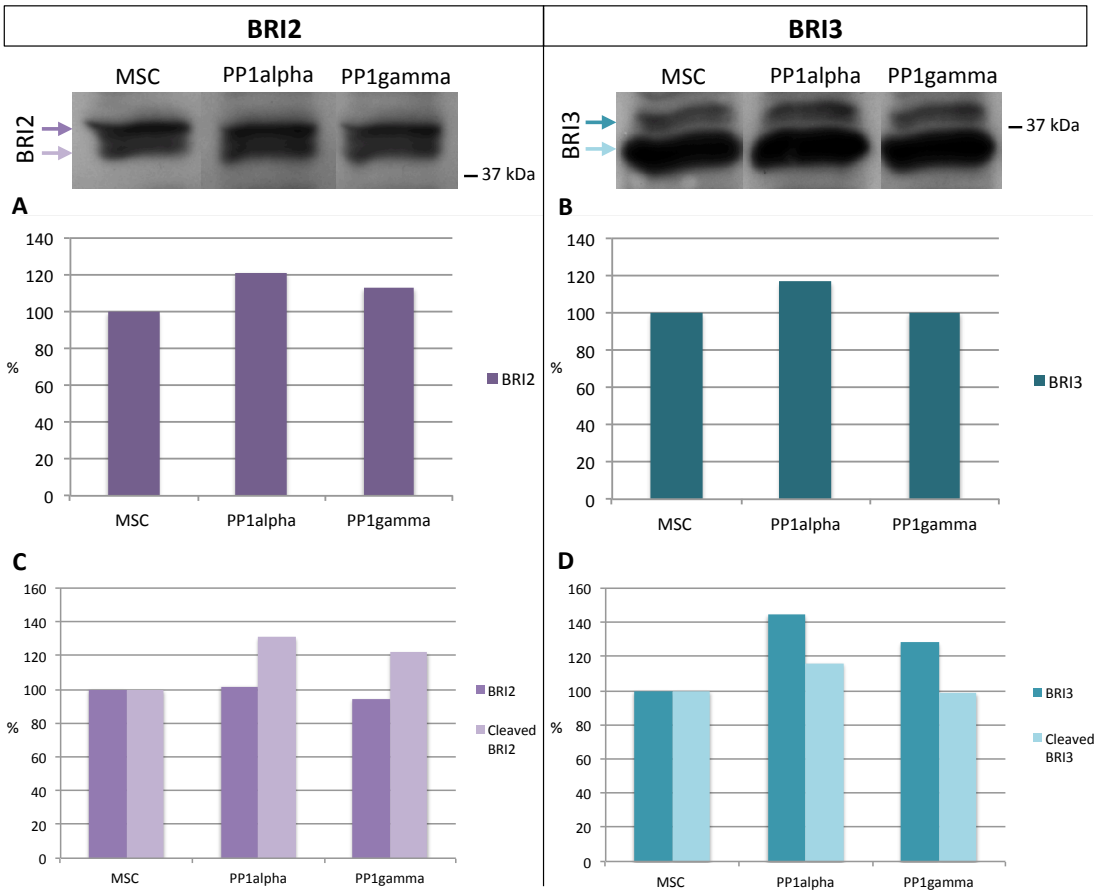

Figure 13 Effects of human PP1alpha and PP1gamma knockdown on total (A and B) and not cleaved and cleaved (C and D) BRI2 (on the left) and BRI3 (on the right) expression. Knockdown was achieved by 48 hours transfection of 3.5 µg of human PP1alpha and PP1gamma shRNA constructs. *MSC, missense control.*

4.3. Generate PP1 Fluorescent GFP/DsRed-Monomer Expression Vectors

In our laboratory we have PP1alpha, PP1gamma1 and PP1gamma2 in pAS2-1 vectors (yeast two-hybrid vector) and we generated PP1alpha, PP1gamma1 and PP1gamma2 fluorescent expression vectors that will be used in further *in vivo* studies. Cloning strategy used was simplified in Figure 14.

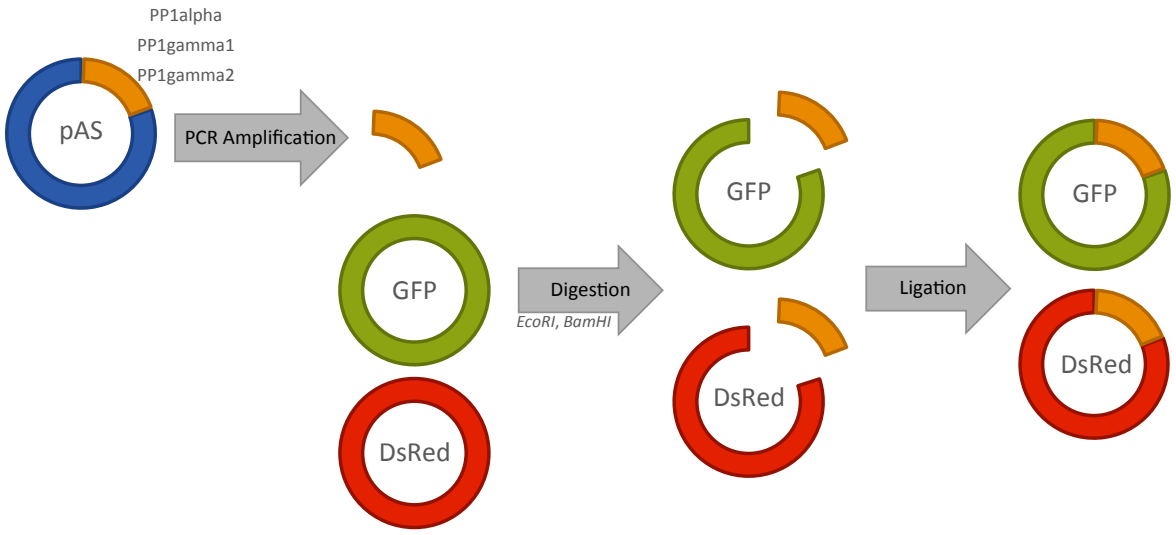

Figure 14 Schematic representation of the cloning strategy for generating PP1alpha-GFP/DsRed-Monomer, PP1gamma1-GFP/DsRed-Monomer and PP1gamma2-GFP/DsRed-Monomer. Orange, inserts: PPalpha, PP1gamma1, P1gamma2; blue, pAS2-1 vector; green, pAcGFP1-C1; red, pDsRed-Monomer-C1. *PCR, polymerase chain reaction.*

Briefly, the three PP1 isoforms were inserted into fluorescent vectors, pAcGFP1-C1 and pDsRed-Monomer-C1, using the restriction enzymes (RE): *EcoRI* and *BamHI*. Thus, PCR amplified PP1alpha, PP1gamma1 and PP1gamma2 (inserts) were further digested with *EcoRI* and *BamHI*. Both vectors were also digested with the same RE. The further ligation of the digested inserts and vectors allows us to generate new PP1alpha, PP1gamma1 and PP1gamma2 expression vectors (Figure 14). The new generated expression vectors were further amplified for further assays.

4.3.1. PCR Amplification of PP1alpha, PP1gamma1 and PP1gamma2

PP1alpha, PP1gamma1 and PP1gamma2 were amplified by PCR from the pAS vectors. Two concentrations (10 ng and 100 ng) of each vector were used for the amplification. To confirm that the DNA was correctly amplified, an agarose gel was performed and the result is presented in Figure 15. PP1alpha, PP1gamma1 and PP1gamma2 coding sequences have the molecular weight of 993bp, 972bp and 1014bp, respectively. Bands corresponding to those sizes are observed in Figure 15.

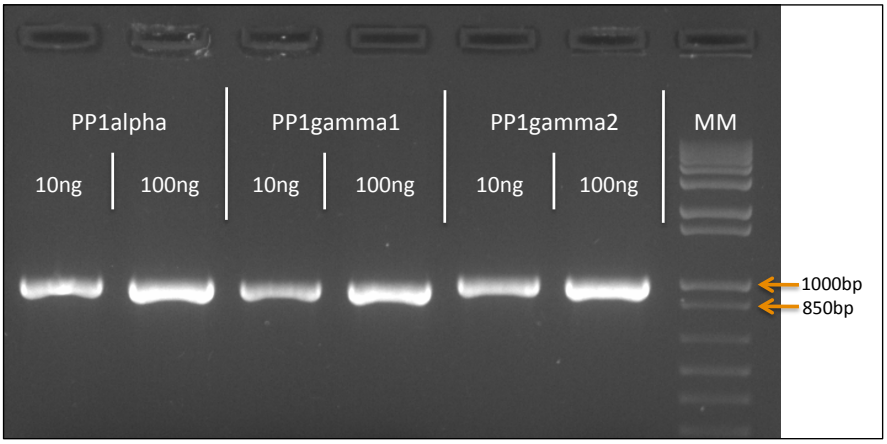

Figure 15 PCR amplification of PP1alpha, PP1gamma1 and PP1gamma2. 1% agarose gel electrophoresis of amplified products using 10 ng and 100 ng of the pAS vectors. The bands observed have around 1000bp corresponding to PP1alpha, PP1gamma1 and PP1gamma2 coding sequences. *MM, Molecular Marker: 1 Kb Plus (Invitrogen™).*

4.3.2. Digestion of the Amplified Products (inserts) and Vectors (GFP/DsRed-Monomer) with *EcoRI* and *BamHI*

The digestion of PCR amplified products (inserts) and vectors was achieved using *EcoRI* and *BamHI*. Upon digestion we performed an agarose gel to observe the digested bands (Figure 16).

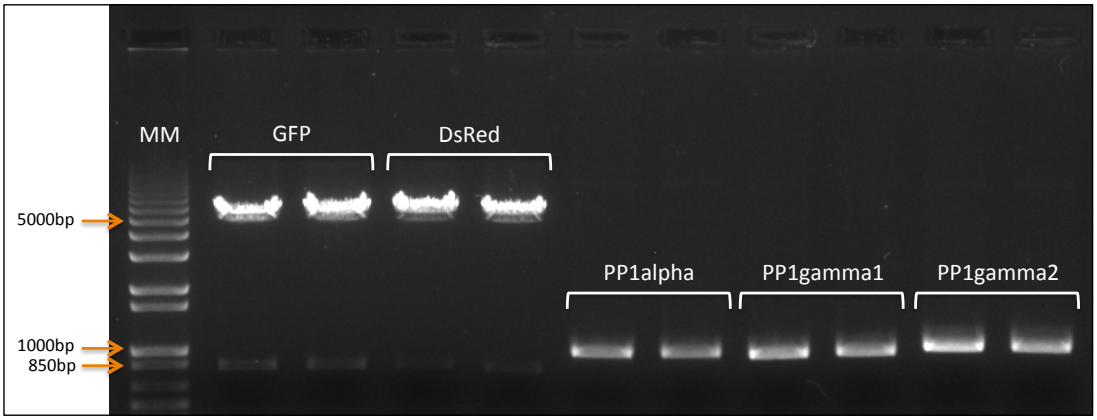

Figure 16 Restriction analysis of vectors (GFP-C1 and DsRes-Monomer-C1) and inserts (PP1 isoforms). After restriction of the vectors, two bands appear in the gel, one referent to the vector, at approximately 5000bp and other referent to BRI2 insert, at approximately 850bp. The PP1 isoforms appear at approximately 1000bp. *MM, Molecular Marker: 1 Kb Plus (Invitrogen™).*

It is possible to observe that DNA digestion was not completely efficient. Therefore, we repeated enzymatic restriction with new *BamHI* and digested only DsRed-Monomer vector and the three PP1 isoforms. DNA was extracted from the gel using *NucleoSpin® Gel and PCR Clean-up Kit* by

Macherey-Nagel and quantified from the agarose gel in Figure 17, using the molecular marker as reference (1650bp band – 40 ng of DNA). The bands in the gel correspond to the vector DsRed-Monomer-C1 with 4700bp and the PP1 isoforms with approximately 1000bp.

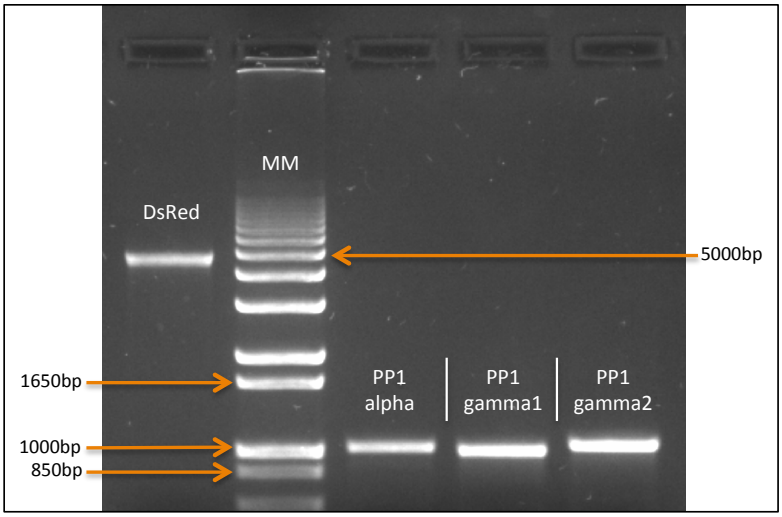

Figure 17 Agarose gel electrophoresis for DNA quantification. DsRed-Monomer-C1 and PP1 isoforms bands have approximately 5000bp and 1000bp, respectively. *MM, Molecular Marker: 1 Kb Plus (Invitrogen™).*

4.3.3. Ligation of Gel Extracted Fragments (inserts and vectors)

Extracted vectors and inserts were used to generate PP1alpha-DsRed-Monomer, PP1gamma1-DsRed-Monomer and PP1gamma2-DsRed-Monomer constructs. Overall, three ligations were performed with 50 ng of vector and vector:insert ratio 1:6. Therefore, it was expected to generate three fluorescent constructs.

4.3.4. Transformation and Analysis of the Positive Clones

After ligation, the putative fluorescent constructs were transformed in *E. coli* XL-1 Blue but no colonies were obtained for PP1gamma2-DsRed-Monomer. The positive clones correspondent to PP1alpha-DsRed-Monomer and PP1gamma1-DsRed-Monomer were isolated by alkaline lysis and analysed by restriction digestion with the endonucleases *EcoRI* and *BamHI*. The resultant fragments were separated by agarose gel electrophoresis to confirm the correct insertion of the PP1 isoforms in DsRed-Monomer-C1 vectors and its sizes. Positive clones were generated for PP1alpha-DsRed-Monomer and PP1gamma1-DsRed-Monomer.

5. Discussion

RNA interference is a natural specific and selective mechanism through which a dsRNA silences the expression of a targeted gene highly homologous to its own sequence, in order to mimic what happens at a cellular level, if a specific gene is weakly expressed. Hence, this technique is a powerful biological tool to study gene function in mammalian cells (Scherr and Eder 2007; Rao *et al.* 2009b). shRNA, a variant of regulatory RNAs, is a small sequence of dsRNA that after being incorporated in cells, uses host machinery and leads to degradation of a specific mRNA sequence, preventing its translation and causing gene knockdown. shRNAs are processed through expression of shRNA vectors as pSIREN-retroQ. The shRNA constructs mediate a strong and long-lasting gene silencing using low copy numbers, which, along with its integration in nuclear and cytoplasmic processing, results in less off-target effects (Rao *et al.* 2009b; Rao *et al.* 2009a). By knocking-down the expression of a specific gene, this method allows the understanding of its physiological function, generating loss-of-function phenotypes, given that this powerful technique was selected to interfere with PP1alpha and PP1gamma (Scherr and Eder 2007; Zhou *et al.* 2010).

PP1 is the major serine/threonine phosphatase and is ubiquitously expressed in all eukaryotic cells as four related isoforms: PP1alpha, PP1beta/delta, PP1gamma1 and PP1gamma2. PP1alpha and PP1gamma1 are highly expressed in brain and PP1gamma2 is testis and spermatozoa enriched (Bollen *et al.* 2010; Peti *et al.* 2012; Chakrabarti *et al.* 2007; Cohen 2002b). PP1 regulates a wide range of cellular processes and its function, subcellular localization and substrate specificity are regulated by the interaction between PP1 catalytic subunit and PP1 binding motifs present in PIPs, and depend on the nature of PIPs (Fardilha *et al.* 2010; Strack *et al.* 1999; Gallego and Virshup 2005; Ulke-Lemée *et al.* 2007). Therefore, PIPs identification and holoenzymes characterization is essential to understand PP1 functions in specific biological pathways (Meiselbach *et al.* 2006; Lee *et al.* 2010). BRI2 and BRI3 belong to a family of integral type II transmembrane glycoproteins with a short cytosolic N-terminal and a large extracellular C-terminal. BRI2 is a highly ubiquitous protein while BRI3 is mainly expressed in brain cells (Vidal *et al.* 2001; Tsachaki *et al.* 2008; Rostagno *et al.* 2005). These two proteins possess RVxF motifs in their intracellular domain, and were lately identified as novel PIPs. Furthermore, it was confirmed that BRI2 and BRI3 interact *in vivo* with both PP1alpha and PP1gamma (Martins et al. 2014, submitted). BRI2 undergoes regulated intramembrane proteolysis, a two-step proteolyitic processing. First, it is processed by a furin and related proteases in the ectodomain, generating a 3 kDa C-terminal peptide. The remaining ectodomain undergoes processing by ADAM-10 and BRICHOS domain, with 25 kDa, is released. The resulting membrane associated N-terminal fragment is cleaved by SPPL2a/2b to produce a 10 kDa intracellular domain and a small secreted

BRI2 C-terminal domain. BRI3 is also processed by furin in its ectodomain, resulting in the secretion of a 3 kDa C-terminal peptide, although it seems that it is not processed by ADAM-10 and SPPL2a/2b. (Tsachaki *et al.* 2008; Wickham *et al.* 2005; Martin *et al.* 2008).

The shRNA constructs for rat and human PP1 used were designed and generated in our laboratory and an optimization of the knockdown efficiency was necessary for future studies related, for instance, with PP1 interactors. In this work, we included studies on the effect of PP1 knockdown on the expression of both BRI2 and BRI3.

In order to establish the best knockdown efficiency of the human PP1alpha and PP1gamma shRNA constructs, transfection in SH-SY5Y neuroblastoma cells was carried out using different conditions. Transfection optimization aims to achieve maximum target gene knockdown efficiency causing minimal cytotoxicity by varying the transfection reagent, amount of DNA and transfection reagent used and exposure time of cells to transfection complexes. We tested two distinct transfection reagents (TurboFect and Lipofectamine), two different DNA concentrations (2 μg and 5 μg) in the preliminary study and an additional one (3.5 μg) in the posterior studies, and two different incubation periods post-transfection (24 hours and 48 hours). A missense oligonucleotide was transfected in the same conditions and used as control. For the resazurin assay purpose, a non-transfected control was used. In the preliminary study, transfection using TurboFect reagent produced, in general, a significant PP1 knockdown. As expected, a reasonable knockdown was achieved 24 hours upon transfection, particularly with 5 μg of DNA since a higher amount of transfected DNA results in more copies of *in vivo* transcribed shRNAs. Surprisingly, no interference in protein expression was observed at 48 hours upon transfection of 2 μg and 5 μg of human PP1alpha shRNA construct. Concerning human PP1gamma, at 48 hours, comparing with 24 hours upon transfection, a higher interference was observed with 5 μg of DNA. It was expected an increase in knockdown efficiency with a higher time of exposure to the transfection complexes. However, a prolonged exposure can cause additional cellular toxicity. Therefore, further studies were necessary to determine with certainty the best transfection conditions.

Results obtained with Lipofectamine reagent show a decrease in human PP1alpha and PP1gamma expression when 5 μg of DNA were transfected. However, this decrease appears to be a consequence of the transfection procedure itself, since the bands obtained for both missense control and shRNA constructs for human PP1 are extremely faded. Thereby, the concentration of Lipofectamine used for transfection may not be adequate for SH-S5Y5 cells and therefore cell viability may be reduced. Besides, at 24 hours upon transfection with Lipofectamine, no decrease

in PP1alpha and PP1gamma expression was observed. When transfection with Lipofectamine was performed using 2 μg of DNA, a reasonable knockdown of human PP1alpha and PP1gamma was observed at 48 hours. Nevertheless, in the preliminary study, TurboFect reagent produced best interference results than Lipofectamine reagent for both human PP1 isoforms, difference that can be explained in part by the mechanism of action of the transfection reagents. The TurboFect/DNA complexes protect DNA from degradation and the rupture of the endocytosed complexes, caused by a rapid osmotic swelling, allows DNA translocation to the nucleus. The mechanism of Lipofectamine reagent is not clearly understood but cells growth, apoptosis and cell cycle may be affected by toxic concentrations of the reagent (Zhong *et al.* 2008). Given that we obtained best results using TurboFect transfection reagent, this was used for the further experiments.

In the following studies, performed with only TurboFect transfection reagent, a new condition, 3.5 μg of DNA, was added once it was not clear which concentration (2 μg and 5 μg) was more suitable, and the post-transfection incubation periods were maintained. Simultaneously, cell viability was assessed by the resazurin assay to ensure that the results obtained were not being influenced by transfection cytotoxicity and consequent cell death. In general, although 30% interference was achieved at 24 hours, knockdown efficiency was clearly better at 48 hours, since a prolonged exposure to the transfection complexes results in more pronounced interference, as long as cell viability levels remain high. Regarding DNA concentration transfected, we concluded that 3.5 μg and 5 μg caused a more pronounced PP1 knockdown, as expected, since higher amounts of transfected DNA generate more *in vivo* transcribed shRNA copies that will silence the specific gene. The maximum interference obtained for both PP1alpha and PP1gamma was approximately 50%, which represents a good protein knockdown.

The resazurin viability assay detects cellular metabolic activity and therefore allowed the determination of cell viability in each sample in comparison with the non-transfected control, which is useful to assess cellular toxicity caused by transfection. As expected, cell viability slightly decreases with time and higher concentrations of transfected DNA, since higher exposure and higher amounts of TurboFect may be toxic. After transfection of missense control and human PP1alpha shRNA constructs, 80% cell viability was observed, which is reasonable considering that foreign nucleic acids are being deliberately introduced into cells causing cellular stress. Transfection of human PP1gama shRNA caused a more pronounced decrease in cell viability, reaching 60%. However, in this case, only two assays were performed (n=2) whereas for the other shRNA constructs, four experiments were performed (n=4). Hence, more cell viability assays

would be necessary to obtain more accurate results concerning human PP1gamma shRNA constructs. Cell viability decrease is similar between samples and missense control, which means it results from the transfection procedure itself. Once the number of viable cells is similar, differences in human PP1alpha and PP1gamma expression is consequence of gene knockdown.

Overall, weighting transfection efficiency and cell viability, we concluded that the best interference efficiency for both human PP1alpha and PP1gamma, was observed at 48 hours upon transfection of 3.5 µg of shRNA construct with TurboFect reagent, with knockdown percentages around 50%. Hence, these were the conditions used to assess BRI2 and BRI3 expression and processing when human PP1alpha and PP1gamma are silenced. The human PP1 knockdown efficiency achieved in this experiment was 20% and 35% for PP1alpha and PP1gamma, respectively, which is considerably lower than the expected interference. Nonetheless, the effects of this moderate knockdown in BRI2 and BRI3 expression were analysed. BRI2 and BRI3 undergo a similar initial processing that consists in the cleavage and release of a small C-terminal peptide of 3 kDa, which explains the presence of two close bands for each protein in the immunoblot: one corresponds to the not cleaved protein and the other to the protein processed (cleaved) by furin. Therefore, we quantified total (two bands together) and also cleaved and uncleaved BRI2 and BRI3 expression levels. Knockdown of human PP1alpha caused a more pronounced interference in total BRI2 and BRI3 expression levels than knockdown of human PP1gamma. More evident differences are observed when the two bands are quantified separately. In the case of BRI2, only the processed protein expression levels were influenced by knockdown of human PP1 whereas in the case of BRI3, the uncleaved protein was more influenced than the processed one. Recent studies in our laboratory described BRI2 and BRI3 as phosphoproteins and proved that PP1 dephosphorylates BRI2 and BRI3 *in vitro* (Martins *et al.* 2014, submitted). Thus, dephosphorylation of both proteins by PP1alpha and PP1gamma may interfere with its processing, however, further studies are necessary to understand this interaction.

For transfection of rat PP1alpha and PP1gamma shRNA constructs in rat cortical cells, only Lipofectamine reagent was used, once it is the recommended reagent for transfection of primary cultures. DNA concentrations and periods post-transfection were the same as the ones used in the preliminary study for human PP1 shRNA constructs. Except for a 40% knockdown of rat PP1alpha 24 hours upon transfection of the shRNA construct, no significant and coherent knockdown was observed. Rat primary neuronal cultures besides presenting a challenge regarding the efficiencies for introducing and expressing exogenous constructs, are very sensitive to

physical stress, temperature, pH and osmolarity alterations (Karra and Dahm 2010). Once the preliminary results did not point to a clear and efficient knockdown of PP1 and rat primary cortical cultures are difficult to obtain and transfect, no additional experiments were performed.

The vectors pAcGFP1-C1 and pDsRed-Monomer-C1 are mammalian expression vectors with 4700bp that, after being transfected into the cells, express proteins detectable by fluorescent microscopy. These fluorescent proteins function as tags for proteins of interest, allowing assessment of its expression and localization. Both vectors contain an *E. coli* kanamycin resistance gene and a MCS with restriction sites for endonucleases *EcoRI* and *BamHI*. In order to generate PP1 fluorescent constructs, three PP1 isoforms (alpha, gamma1 and gamma2) were inserted in both GFP-C1 and DsRed-Monomer-C1 vectors through PCR subcloning, which includes amplification of the interest fragment by PCR, purification of the PCR products, ligation of the proteins to the new vector and finally transformation of the ligation in bacteria. We successfully generated PP1alpha-DsRed-Monomer and PP1gamma1-DsRed-Monomer fluorescent vectors that will be fully sequenced.

Initially we had some difficulties in DNA digestion, possibly due to *BamHI* enzyme efficiency. After digestion with the two endonucleases, small fragments of the vectors MCS and inserts ends are separated from the fragments of interest but are not detectable in an agarose gel. In the case of the inserts, the bands obtained before and after the process of digestion are identical, thus, it was not possible to assure that the DNA was well digested. Vectors GFP-C1 and DsRed-Monomer-C1 used had no insert, thus it was possible to verify if the vector was linearized or not but it was not possible to differentiate vector cut with only one enzyme from vector cut with two. Hence, a problem with one of the restriction enzymes would not be detected and would impair posterior ligation. Later, vectors GFP-C1 and DsRed-Monomer-C1 containing BRI2 were used to facilitate post-digestion agarose gel analysis. The results obtained indicate that in fact digestion was not efficient once three bands were observed in the gel, correspondent to the removed insert, the linearized vector with insert and without it. Since digestion of the vectors is impaired, it is likely that the PP1 inserts are not completely digested, neither. In conclusion, after digestion, the samples contain both cut and uncut DNA and consequently, only a small amount of cut vector and insert is available for ligation. In further experiments performed with new *BamHI* enzyme to digest DsRed-Monomer vector and PP1alpha and PP1gamma1 inserts, we achieved better results upon DNA digestion and several colonies were obtained and analysed after transformation,

confirming the presence of positive clones of PP1alpha-DsRed-Monomer and PP1gamma1-DsRed-Monomer. The remaining constructs (PP1gamma2-DsRed-Monomer, PP1alpha-FGP, PP1gamma1-GFP and PP1gamma2-GFP) will be produced in the future.

The PP1 fluorescent constructs will be used to determine co-localization of PP1 isoforms with BRI2 and BRI3 and assess protein expression and localization. *In vivo* studies will contribute to the understanding and characterization of the PP1:BRI complexes.

6. Conclusion and Future Perspectives

From the shRNA optimization study, we concluded that the best interference efficiency was achieved 48 hours upon transfection of 3.5 μg of both human PP1alpha and PP1gamma shRNA constructs using TurboFect, with PP1 knockdown around 50%. Total BRI2 and BRI3 extracellular levels do not appear to be influenced by human PP1alpha and PP1gamma knockdown. However, it is likely that PP1 is involved in BRI2 and BRI3 processing. Further studies are required to validate these results and understand how human PP1 affects BRI2 and BRI3 processing.

Regarding production of PP1 fluorescent constructs, besides the holdbacks during the cloning procedure, PP1alpha-DsRed-Monomer and PP1gamma-DsRed-Monomer were successfully generated.

The future perspectives of this work are the following:

- Evaluate human PP1alpha and PP1gamma expression and cellular localization by immunocytochemistry upon knockdown;
- Validate results obtained for effects of human PP1alpha and PP1gamma knockdown on BRI2 and BRI3 processing and expression levels, and determine the effects on BRI2 and BRI3 localization;
- Determine the co-localization of the three PP1 isoforms with BRI2 and BRI3 and assess protein expression and localization.
- Generate PP1gamma2-DsRed-Monomer, PP1alpha-GFP, PP1gamma1-GFP and PP1gamma2-GFP.

7. References

Aggen, J.B., Nairn, A.C. and Chamberlin, R., 2000. Regulation of protein phosphatase-1. *Chemistry & Biology*, 7(1), pp.13–23.

Allen, P.B., Ouimet, C.C. and Greengard, P., 1997. Spinophilin, a novel protein phosphatase 1 binding protein localized to dendritic spines. *Proceedings of the National Academy of Sciences of the United States of America*, 94(18), pp.9956–61.

Andreassen, P.R., Lacroix, F.B., Villa-Moruzzi, E. and Margolis, R.L., 1998. Differential Subcellular Localization of Protein Phosphatase-1 alpha, gamma1, and delta Isoforms during Both Interphase and Mitosis in Mammalian Cells. *The Journal of Cell Biology*, 141(5), pp.1207–15.

Barford, D., Das, A.K. and Egloff, M.-P., 1998. The Structure and Mechanism of Protein Phosphatases: Insights into Catalysis and Regulation. *Annual Review of Biophysics and Biomolecular Structure*, 27, pp.133–64.

Bernstein, E., Caudy, A.A., Hammond, S.M. and Hannon, G.J., 2001. Role for a bidentate ribonuclease in the initiation step of RNA interference. *Nature*, 409(6818), pp.363–6.

Bollen, M., 2001. Combinatorial control of protein phosphatase-1. *Trends in Biochemical Sciences*, 26(7), pp.426–431.

Bollen, M., Peti, W., Ragusa, M.J. and Beullens, M., 2010. The extended PP1 toolkit: designed to create specificity. *Trends in Biochemical Sciences*, 35(8), pp.450–8. at <http://www.pubmedcentral.nih.gov/articlerender.fcgi?artid=3131691&tool=pmcentrez&rendertype=abstract> [Accessed July 9, 2014].

Bridge, A.J., Pebernard, S., Ducraux, A., Nicoulaz, A.-L. and Iggo, R., 2003. Induction of an interferon response by RNAi vectors in mammalian cells. *Nature Genetics*, 34(3), pp.263–4.

Brummelkamp, T.R., Bernards, R. and Agami, R., 2002. A System for Stable Expression of Short Interfering RNAs in Mammalian Cells. *Science*, 296(5567), pp.550–3.

Ceulemans, H. and Bollen, M., 2004. Functional Diversity of Protein Phosphatase-1, a Cellular Economizer and Reset Button. *Physiological Reviews*, 84(1), pp.1–39.

Ceulemans, H., Stalmans, W. and Bollen, M., 2002. Regulator-driven functional diversification of protein phosphatase-1 in eukaryotic evolution. *BioEssays*, 24(4), pp.371–81.

Chakrabarti, R., Kline, D., Lu, J., Orth, J., Pilder, S. and Vijayaraghavan, S., 2007. Analysis of Ppp1cc-Null Mice Suggests a Role for PP1gamma2 in Sperm Morphogenesis. *Biology of Reproduction*, 76(6), pp.992–1001.

Chendrimada, T.P., Gregory, R.I., Kumaraswamy, E., Cooch, N., Nishikura, K. and Shiekhattar, R., 2005. TRBP recruits the Dicer complex to Ago2 fro microRNA processing and gene silencing. *Nature*, 436(7051), pp.740–4.

Choi, S.-I., Vidal, R., Frangione, B. and Levy, E., 2004. Axonal transport of British and Danish amyloid peptides via secretory vesicles. *The FASEB Journal*, 18(2), pp.373–5.

Choi, S.C., Kim, J., Kim, T.H., Cho, S.Y., Park, S.S., Kim, K.D. and Lee, S.H., 2001. Cloning and Characterization of a Type II Integral Transmembrane Protein Gene, Itm2c, That Is Highly Expressed in the Mouse Brain. *Molecules and Cells*, 12(3), pp.391–7.

Cohen, P., 2002a. Protein kinases--the major drug targets of the twenty-first century? *Nature Reviews Drug Discovery*, 1(4), pp.309–15.

Cohen, P., 1989. The structure and regulation of protein phosphatases. *Annual Review of Biochemistry*, 58, pp.453–508.

Cohen, P.T.W., 1997. Novel protein serine/threonine phosphatases: variety is the spice of life. *Trends in Biochemical Sciences*, 22(7), pp.245–51.

Cohen, P.T.W., 2002b. Protein phosphatase 1 - targeted in many directions. *Journal of Cell Science*, 115(Pt 2), pp.241–56.

Cruz e Silva, E.F. da, Fox, C.A., Ouimet, C.C., Gustafson, E., Watson, S.J. and Greengard, P., 1995. Differential Expression of Protein Phosphatase 1 Isoform in Mammalian Brain. *The Journal of Neuroscience*, 15(5), pp.3375–89.

Egloff, M., Cohen, P.T.W., Reinemer, P. and Barford, D., 1995. Crystal Structure of the Catalytic Subunit of Human Protein Phosphatase 1 and its Complex with Tungstate. *Journal of Molecular Biology*, 1(254), pp.942–59.

Egloff, M.-P., Johnson, D.F., Moorhead, G., Cohen, P.T.W., Cohen, P. and Barford, D., 1997. Structural basis for the recognition of regulatory subunits by the catalytic subunit of protein phosphatase 1. *The EMBO journal*, 16(8), pp.1876–87.

Elbashir, S.M., Lendeckel, W. and Tuschl, T., 2001. RNA interference is mediated by 21- and 22-nucleotide RNAs. *Genes & Development*, 15(2), pp.188–200.

Esteves, S.L.C., Domingues, S.C., da Cruz e Silva, O.A.B., Fardilha, M. and da Cruz e Silva, E.F., 2012. Protein Phosphatase 1α Interacting Proteins in the Human Brain. *OMICS*, 16(1-2), pp.3–17.

Fardilha, M., Esteves, S.L.., Korrodi-Gregório, L., da Cruz e Silva, O.A.B. and da Cruz e Silva, E.F., 2010. The Physiological Relevance of Protein Phosphatase 1 and its Interacting Proteins to Health and Disease. *Current Medicinal Chemistry*, 17(33), pp.3996–4017.

Fardilha, M., Esteves, S.L.C., Korrodi-Gregório, L., Vintém, A.P., Domingues, S.C., Rebelo, S., Morrice, N., Cohen, P.T.W., da Cruz e Silva, O. a B. and da Cruz e Silva, E.F., 2011. Identification of the human testis protein phosphatase 1 interactome. *Biochemical Pharmacology*, 82(10), pp.1403–15.

Gallego, M. and Virshup, D.M., 2005. Protein serine/threonine phosphatases: life, death, and sleeping. *Current Opinion in Cell Biology*, 17(2), pp.197–202.

Ghiso, J., Rostagno, A., Tomidokoro, Y., Lashley, T., Bojsen-Møller, M., Braendgaard, H., Plant, G., Holton, J., Lal, R., Revesz, T. and Frangione, B., 2006. Genetic Alterations of the BRI2 gene: Familial British and Danish Dementias. *Brain Pathology*, 16(1), pp.71–9.

Green, A.A. and Cori, G.T., 1943. Crystalline Muscle Phosphorylase: II. Prosthetic Group. *The Journal*, 151, pp.31–8.

Hammond, S.M., Boettcher, S., Caudy, A.A., Kobayashi, R. and Hannon, G.J., 2001a. Argonaute2, a Link Between Genetic and Biochemical Analyses of RNAi. *Science*, 293(5532), pp.1146–50.

Hammond, S.M., Caudy, A.A. and Hannon, G.J., 2001b. Post-transcriptional gene silencing by double-stranded RNA. *Nature Reviews Genetics*, 2(2), pp.110–9.

Hannon, G.J. and Conklin, D.S., 2004. RNA Interference by Short Hairpin RNAs Expressed in Vertebrate Cells. *Methods in Molecular Biology*, 257, pp.255–66.

Hendrickx, A., Beullens, M., Ceulemans, H., Den Abt, T., Van Eynde, A., Nicolaescu, E., Lesage, B. and Bollen, M., 2009. Docking Motif-Guided Mapping of the Interactome of Protein Phosphatase-1. *Chemistry & Biology*, 16(4), pp.365–71.

Heroes, E., Lesage, B., Görnemann, J., Beullens, M., Van Meervelt, L. and Bollen, M., 2013. The PP1 binding code: a molecular-lego strategy that governs specificity. *The FEBS Journal*, 280(2), pp.584–95.

Holmes, C.F.B., Campbell, D.G., Caudwell, F.B., Aitken, A. and Cohen, P., 1986. The protein phosphatases involved in cellular regulation. Primary structure of inhibitor-2 from rabbit skeletal muscle. *European Journal of Biochemistry*, 155(1), pp.173–82.

Honkanen, R.E. and Golden, T., 2002. Regulators of serine/threonine protein phosphatases at the dawn of a clinical era? *Current Medicinal Chemistry*, 9(22), pp.2055–75.

Huang, F.L. and Glinsmann, W., 1976. A second heat-stable protein inhibitor of phosphorylase phosphatase from rabbit muscle. *FEBS Letters*, 62(3), pp.326–29.

Huang, H., Horiuchi, A., Watanabe, T., Shih, S.-R., Tsay, H.-J., Li, H.-C., Greengard, P. and Nairn, A.C., 1999. Characterization of the Inhibition of Protein Phosphatase-1 by DARPP-32 and Inhibitor-2. *Journal of Biological Chemistry*, 274(12), pp.7870–8.

Huang, Z. and Vijayaraghavan, S., 2004. Increased Phosphorylation of a Distinct Subcellular Pool of Protein Phosphatase, PP1gamma2, During Epididymal Sperm Maturation. *Biology of Reproduction*, 70(2), pp.439–47.

Hunter, T., 1995. Protein Kinases and Phosphatases: The Yin and Yang of Protein Phosphorylation and Signaling. *Cell*, 80(2), pp.225–36.

Hutvágner, G. and Zamore, P.D., 2002. RNAi : nature abhors a double-strand. *Current Opinion in Genetics & Development*, 12(2), pp.225–32.

Ishihara, H., Martin, B.L., Brautigan, D.L., Karaki, H., Ozaki, H., Kato, Y., Fusetani, N., Watabe, S., Hashimoto, K., Uemura, D. and Hartshorne, D.J., 1989. Calyculin A and Okadaic Acid: Inhibitors of Protein Phosphatase activity. *Biochemical and Biophysical Research Communications*, 159(3), pp.871–7.

Karra, D. and Dahm, R., 2010. Transfection Techniques for Neuronal Cells. *The Journal of neuroscience*, 30(18), pp.6171–7.

Killilea, D.S., Mellgren, R.L., Aylward, J.H., Metieh, M.E. and Lee, E.Y.C., 1979. Liver Protein Phosphatases : Studies of the Presumptive Native Forms of Phosphorylase Phosphatase Activity in Liver Extracts and Their Dissociation to a Catalytic Subunit of Mr 35,000. *Archives of Biochemistry and Biophysics*, 193(1), pp.130–9.

Kunkel, G.R. and Pederson, T., 1989. Transcription of a human U6 small nuclear RNA gene in vivo withstands deletion of intragenic sequences but not of an upstream TATATA box. *Nucleic Acids Research*, 17(18), pp.7371–9.

Kutuzov, M.A., Solov'eva, O. V, Andreeva, A. V and Bennett, N., 2002. Protein Ser/Thr phosphatases PPEF interact with calmodulin. *Biochemical and Biophysical Research Communications*, 293(3), pp.1047–52.

Lee, J.-H., You, J., Dobrota, E. and Skalnik, D.G., 2010. Identification and Characterization of a Novel Human PP1 Phosphatase Complex. *The Journal of Biological Chemistry*, 285(32), pp.24466–76.

Life Technologies, 2014. siRNA Expression Vectors with Selectable Markers For Long Term Studies in Mammalian Cells. at <http://www.lifetechnologies.com/content/dam/LifeTech/migration/en/images/ics-

organized/applications/nucleic-acid-purification/data-image/560-wide.par.11963.image.560.614.1..gif> [Accessed August 28, 2014].

Mackintosh, C. and Klumpp, S., 1990. Tautomycin from the bacterium Streptomyces verticillatus. Another potent and specific inhibitor of protein phosphatases 1 and 2A. *FEBS Letters*, 277(1-2), pp.137–40.

Martin, L., Fluhrer, R., Reiss, K., Kremmer, E., Saftig, P. and Haass, C., 2008. Regulated Intramembrane Proteolysis of Bri2 (Itm2b) by ADAM10 and SPPL2a/SPPL2b. *The Journal of Biological Chemistry*, 283(3), pp.1644–52.

Martins, F., Rebelo, S., Santos, M., Cotrim, C.Z., da Cruz e Silva, E.F. and da Cruz e Silva, O.A.B., 2014. BRI2 and BRI3 are two novel PP1 regulatory proteins. *Biochemistry*.

Matsuda, S., Giliberto, L., Matsuda, Y., McGowan, E.M. and D'Adamio, L., 2008. BRI2 Inhibits Amyloid beta-Peptide Precursor Protein Processing by Interfering with the Docking of Secretases to the Substrate. *The Journal of Neuroscience*, 28(35), pp.8668–76.

Matsuda, S., Matsuda, Y. and D'Adamio, L., 2009. BRI3 Inhibits Amyloid Precursor Protein Processing in a Mechanistically Distinct Manner from Its Homologue Dementia Gene BRI2. *Journal of Biological Chemistry*, 284(23), pp.15815–25.

Meiselbach, H., Sticht, H. and Enz, R., 2006. Structural Analysis of the Protein Phosphatase 1 Docking Motif: Molecular Description of Binding Specificities Identifies Interacting Proteins. *Chemistry & Biology*, 13(1), pp.49–59.

Mellgren, R.L., Aylward, J.H., Killilea, D.S. and Lee, E.Y.C., 1979. The Activation and Dissociation of a Native High Molecular Weight Form of Rabbit Skeletal Muscle Phosphorylase Phosphatase by Endogenous Ca2+-dependent Proteases. *The Journal of Biological Chemistry*, 254(3), pp.648–52.

Mi, J., Guo, C., Brautigan, D.L. and Larner, J.M., 2007. Protein Phosphatase-1alpha Regulates Centrosome Splitting through Nek2. *Cancer Research*, 67(3), pp.1082–9.

Moore, C.B., Guthrie, E.H., Huang, M.T. and Taxman, D.J., 2010. Short Hairpin RNA (shRNA): Design, Delivery, and Assessment of Gene Knockdown M. Sioud, ed. *Methods in Molecular Biology*, 629, pp.141–58.

Moorhead, G.B.G., De Wever, V., Templeton, G. and Kerk, D., 2009. Evolution of protein phosphatases in plants and animals. *The Biochemical journal*, 417(2), pp.401–9.

NCBIa, 2014. Homo sapiens protein phosphatase 1, catalytic subunit, alpha isozyme (PPP1CA), transcript variant 1, mRNA. at <http://www.ncbi.nlm.nih.gov/nuccore/nm_002708.3> [Accessed April 12, 2014].

NCBIb, 2014. Homo sapiens protein phosphatase 1, catalytic subunit, gamma isozyme (PPP1CC), transcript variant 1, mRNA. at <http://www.ncbi.nlm.nih.gov/nuccore/nm_002710> [Accessed April 12, 2014].

NCBIc, 2014. Homo sapiens protein phosphatase 1, catalytic subunit, gamma isozyme (PPP1CC), transcript variant 2, mRNA. at <http://www.ncbi.nlm.nih.gov/nuccore/nm_001244974> [Accessed April 12, 2014].

Nykänen, A., Haley, B. and Zamore, P.D., 2001. ATP Requirements and Small Interfering RNA structure in the RNA Interference Pathway. *Cell*, 107(3), pp.309–21.

Paddison, P.J., Caudy, A.A., Bernstein, E., Hannon, G.J. and Conklin, D.S., 2002. Short hairpin RNAs (shRNAs) induce sequence-specific silencing in mammalian cells. *Genes & Development*,

16(8), pp.948–58. at <http://www.pubmedcentral.nih.gov/articlerender.fcgi?artid=152352&tool=pmcentrez&rendertype=abstract> [Accessed July 15, 2014].

Paul, C.P., Good, P.D., Winer, I. and Engelke, D.R., 2002. Effective expression of small interfering RNA in human cells. *Nature Biotechnology*, 20(5), pp.505–8.

Peti, W., Nairn, A.C. and Page, R., 2012. Structural basis for protein phosphatase 1 regulation and specificity. *The FEBS Journal*, 280(2013), pp.596–611.

Rao, D.D., Senzer, N., Cleary, M.A. and Nemunaitis, J., 2009a. Comparative assessment of siRNA and shRNA off target effects: what is slowing clinical development. *Cancer Gene Therapy*, 16(11), pp.807–9.

Rao, D.D., Vorhies, J.S., Senzer, N. and Nemunaitis, J., 2009b. siRNA vs. shRNA: Similarities and Differences. *Advanced Drug Delivery Reviews*, 61(9), pp.746–59.

Rostagno, A., Tomidokoro, Y., Lashley, T., Ng, D., Plant, G., Holton, J., Frangione, B., Revesz, T. and Ghiso, J., 2005. Chromosome 13 dementias. *Cellular and Molecular Life Sciences*, 62(16), pp.1814–25.

Santos, M., 2014. *Characterization of novel LAP1 complexes and their relevance in DYT1 dystonia*. University of Aveiro.

Scherr, M. and Eder, M., 2007. Gene Silencing by Small Regulatory RNAs in Mammalian Cells. *Cell Cycle*, 6(4), pp.444–9.

Shi, Y., 2009. Serine/Threonine Phosphatases: Mechanism through Structure. *Cell*, 139(3), pp.468–84.

Sledz, C.A., Holko, M., de Veer, M.J., Silverman, R.H. and Williams, B.R.G., 2003. Activation of the interferon system by short-interfering RNAs. *Nature Cell Biology*, 5(9), pp.834–9.

Strack, S., Kini, S., Ebner, F.F., Wadzinski, B.E. and Colbran, R.J., 1999. Differential Cellular and Subcellular Localization of Protein Phosphatase 1 Isoforms in Brain. *The Journal of Comparative Neurology*, 413(3), pp.373–84.

Sugiyama, G., Takeuchi, H., Nagano, K., Gao, J., Ohyama, Y., Mori, Y. and Hirata, M., 2012. Regulated Interaction of Protein Phosphatase 1 and Protein Phosphatase 2A with Phospholipase C-Related but Catalytically Inactive Protein. *Biochemistry*, 51(16), pp.3394–403.

Sui, G., Soohoo, C., Affar, E.B., Gay, F., Shi, Y., Forrester, W.C. and Shi, Y., 2002. A DNA vector-based RNAi technology to suppress gene expression in mammalian cells. *Proceedings of the National Academy of Sciences of the United States of America*, 99(8), pp.5515–20.

Sutherland, E.W.J. and Wosilait, W.D., 1955. Inactivation and Activation of Liver Phosphorylase. *Nature*, 175(4447), pp.169–70.

Tanuma, N., Kim, S.-E., Beullens, M., Tsubaki, Y., Mitsuhashi, S., Nomura, M., Kawamura, T., Isono, K., Koseki, H., Sato, M., Bollen, M., Kikuchi, K. and Shima, H., 2008. Nuclear Inhibitor of Protein Phosphatase-1 (NIPP1) Directs Protein Phosphatase-1 (PP1) to Dephosphorylate the U2 Small Nuclear Ribonucleoprotein Particle (snRNP) Component, Spliceosome-associated Protein 155 (Sap155). *The Journal of Biological Chemistry*, 283(51), pp.35805–14.

Terrak, M., Kerff, F., Langsetmo, K. and Tao, T., 2004. Structural basis of protein phosphatase 1 regulation. *Nature*, 429(6993), pp.780–4.

Trinkle-Mulcahy, L., Sleeman, J.E. and Lamond, A.I., 2001. Dynamic targeting of protein phosphatase 1 within the nuclei of living mammalian cells. *Journal of Cell Science*, 114(23), pp.4219–28.

Tsachaki, M., Ghiso, J. and Efthimiopoulos, S., 2008. BRI2 as a central protein involved in neurodegeneration. *Biotechnology journal*, 3(12), pp.1548–54.

Ulke-Lemée, A., Trinkle-Mulcahy, L., Chaulk, S., Bernstein, N.K., Morrice, N., Glover, M., Lamond, A.I. and Moorhead, G.B.G., 2007. The nuclear PP1 interacting protein ZAP3 (ZAP) is a putative nucleoside kinase that complexes with SAM68, CIA, NF110/45, and HNRNP-G. *Biochimica et Biophysica Acta*, 1774(10), pp.1339–50.

Uniprot, 2014. P62136- PP1A_HUMAN. at <http://www.uniprot.org/uniprot/P62136> [Accessed April 15, 2014].

Vidal, R., Calero, M., Révész, T., Plant, G., Ghiso, J. and Frangione, B., 2001. Sequence, genomic structure and tissue expression of Human BRI3, a member of the BRI gene family. *Gene*, 266(1-2), pp.95–102.

Wakula, P., Beullens, M., Ceulemans, H., Stalmans, W. and Bollen, M., 2003. Degeneracy and Function of the Ubiquitous RVXF Motif That Mediates Binding to Protein Phosphatase-1. *The Journal of Biological Chemistry*, 278(21), pp.18817–23.

Wakula, P., Beullens, M., van Eynde, A., Ceulemans, H., Stalmans, W. and Bollen, M., 2006. The translation initiation factor eIF2beta is an interactor of protein phosphatase-1. *The Biochemical journal*, 400(Pt 2), pp.377–83.

Wang, B., Zhang, P. and Wei, Q., 2008. Recent progress on the structure of Ser/Thr protein phosphatases. *Science in China Series C: Life Sciences*, 51(6), pp.487–94.

Wickham, L., Benjannet, S., Marcinkiewicz, E., Chretien, M. and Seidah, N.G., 2005. Beta-Amyloid protein converting enzyme 1 and brain-specific type II membrane protein BRI3: binding partners processed by furin. *Journal of Neurochemistry*, 92(1), pp.93–102.

Yi, R.U.I., Doehle, B.P., Qin, Y.I., Macara, I.A.N.G. and Cullen, B.R., 2005. Overexpression of Exportin 5 enhances RNA interference mediated by short hairpin RNAs and microRNAs. *RNA*, 11(2), pp.220–6.

Yu, J.-Y., DeRuiter, S.L. and Turner, D.L., 2002. RNA interference by expression of short-interfering RNAs and hairpin RNAs in mammalian cells. *Proceedings of the National Academy of Sciences of the United States of America*, 99(9), pp.6047–52.

Zhong, Y.Q., Wei, J., Fu, Y.R., Shao, J., Liang, Y.W., Lin, Y.H., Liu, J. and Zhu, Z.H., 2008. Toxicity of cationic liposome Lipofectamine 2000 in human pancreatic cancer Capan-2 cells. *Nan Fang yi ke da xue xue bao = Journal of Southern Medical University*, 28(11), pp.1981–4.

Zhou, F., Malik, F.A., Yang, H., Li, X., Roy, B. and Miao, Y., 2010. Application of short hairpin RNAs (shRNAs) to study gene function in mammalian systems. *African Journal of Biotechnology*, 9(54), pp.9086–91.

Appendix

I. Culture media and solutions

a. Bacteria Media

LB (Luria-Bertrani) Medium

To 950 mL of deionised H_2O add:

LB 25 g

Agar 15 g (for plates only)

Shake until solutes have dissolved. Adjust the volume of the solution to 1 L with deionised H_2O. Sterilize by autoclaving.

SOB Medium

To 950 mL of deionised H_2O add:

SOB Broth 25.5 g

Shake until the solutes have dissolved. Add 10 mL of a 250 mM KCl (prepared by dissolving 1.86 g of KCl in 100 mL of dieonised H_2O). Adjust the pH to 7.0 with 5 N NaOH. Just prior to use add 5 mL of sterile solution of 2 M $MgCl_2$ (prepared by dissolving 19 g of $MgCl_2$ in 90 mL of deionised H_2O). Adjust the volume of the solution to 1 L with deionised H_2O and sterilize by autoclaving).

SOC Medium

SOC is identical to SOB except that it contains 20 mM glucose. After the SOB medium has been autoclaved, allow it to cool to 60°C and add 20 mL of a sterile 1 M glucose (this solution is made by dissolving 18 g of glucose in 90 mL of deionised H_2O; after the sugar has dissolved, adjust the volume of the solution to 1 L with deionised H_2O and sterilize by filtration through a 0.22-micron filter).

Antibiotics

Ampicilin 50 µg/µL

Kanamycin 30 µg/µL

b. Cell Culture Solutions and Immunocytochemistry

SH-SY5Y Complete Medium

To 600 mL of deionised H_2O add:

MEM	4.805 g
F12	5.315 g
Sodium pyruvate	0.055 g
Sodium bicarbonate	1.5 g
AA	10 mL
L-glutamine	2.5 mL

Mix until the solutes have dissolved. Adjust the pH to 7.2-7.4 and add:

FBS	100 mL

Adjust the volume to 1 L with deionised H_2O, filter through a 0.2 µm filter and store at 4°C.

10 mg/mL Poly-D-lysine stock (100x)

In 10 mL of deionised deionised H_2O dissolve 100 mg of poly-D-lysine.

Borate Buffer

In 1 L of deionised H_2O dissolve 9.28 g of boric acid. Adjust to pH 8.2, sterilize by filtering through a 0.2 µM filter and store at 4°C.

Poly-D-lysine Solution

To a final volume of 100 mL, dilute 1 mL of the 10 mg/mL poly-D-lysine stock solution in borate buffer.

Hank's Balanced Salt Solution (HBSS)

In deionised H_2O dissolve:

NaCl	137 mM
KCl	5.36 mM
KH_2PO_4	0.44 mM
$Na_2HPO_42H_2O$	0.34 mM
$NaHCO_3$	4.16 mM
Glucose	5 mM
Sodium pyruvate	1 mM
HEPES	10 mM

Adjust to pH 7.4, sterilize by filtering through a 0.2 µm filter and store at 4°C.

Complete Neurobasal medium

This serum-free medium is supplemented with:

B27 supplement	2%
L-glutamine	0.5 mM
Gentamicin	60 µg/mL
Phenol Red	0.001%

Adjust to pH 7.4, sterilize by filtering through a 0.2 µm filter and store at 4°C.

1x Phosphate Buffered Saline (PBS)

For a final volume of 500 mL, dissolve one pack of BupH Modified Dulbecco's Phosphate Buffered Saline Pack (*Pierce*) in deionised H_2O. Final composition:

Sodium Phosphate	8 mM
Potassium Phosphate	2 mM
NaCl	40 mM
KCl	10 mM

Sterilize by filtering through a 0.2 µm filter and store at 4°C.

4% Paraformaldehyde

To 25 mL of deionised H_2O add:

Paraformaldehyde 4 g

Dissolve by heating the mixture at 58°C while stirring. Add 1-2 drops of 1 M NaOH to clarify the solution and filter through a 0.2 µm filter. Add 50 mL of 2x PBS and adjust the volume to 100 mL with deionised H_2O.

c. SDS-PAGE and Immunoblotting Solutions

Lower Gel Buffer (LGB) (4x)

To 900 mL of deionised H_2O add:

Tris 181.65 g

SDS 4 g

Mix until the solutes have dissolved. Adjust the pH to 8.9 and adjust the volume to 1 L with deionised H_2O.

Upper Gel Buffer (UGB) (5x)

To 900 mL of deionised H_2O add:

Tris 75.69 g

Mix until the solute has dissolved. Adjust the pH to 6.8 and adjust the volume to 1 L with deionised H_2O.

30% Acrylamide/0.8% Bisacrylamide

To 70 mL of deionised H_2O add:

Acrylamide 29.2 g

Bisacrylamide 0.8 g

Mix until the solutes have dissolved. Adjust the volume to 100 mL with deionised H_2O. Filter through a 0.2 µm filter and store at 4°C.

10% Ammonium Persulfate (APS)

In 10 mL of deionised H_2O dissolve 1 g of APS.

10% Sodium Dodecilsulfate (SDS)

In 10 mL of deionised H_2O dissolve 1 g of SDS.

Loading Gel Buffer (4x)

1 M Tris solution (pH 6.8)	2.5 mL (250 mM)
SDS	0.8 g (8%)
Glycerol	4 mL (40%)
β-Mercaptoethanol	2 mL (2%)
Bromophenol blue	1 mg (0.01%)

Adjust the volume to 10 mL with deionised H_2O. Store in darkness at room temperature.

1 M Tris (pH 6.8) Solution

To 150 mL of deionised H_2O add:

Tris base 30.3 g

Adjust the pH to 6.8 and adjust the final volume to 250 mL.

10x Running Buffer

Tris	30.3 g (250 mM)
Glycine	144.2 g (2.5 M)
SDS	10 g (1%)

Dissolve in deionised H_2O, adjust the pH to 8.3 and adjust the volume to 1 L.

1x Transfer buffer

Tris 3.03 g (25 mM)

Glycine 14.41 g (192 mM)

Mix until solutes dissolution. Adjust the pH to 8.3 with HCl and adjust the volume to 800 mL with deionised H_2O. Just prior to use add 200 mL of methanol (20%).

10x Tris Buffered Saline (TBS)

Tris 12.11 g (10 mM)

NaCl 87.66 g (150 mM)

Adjust the pH to 8.0 with HCl and adjust the volume to 1 L with deionised H_2O.

10x TBS+Tween (TBST)

Tris 12.11 g (10 mM)

NaCl 87.66 g (150 mM)

Tween 20 5 mL (0.05%)

Adjust the pH to 8.0 with HCl and adjust the volume to 1 L with deionised H_2O.

Developer Solution

GBX developer 220 mL

Adjust the volume to 1 L with deionized H_2O.

Fixation Solution

GBX fixer 220 mL

Adjust the volume to 1 L with deionized H_2O.

Membranes Stripping Solution

Tris.HCl	3.76 g (62.5 mM)
SDS	10 g (2%)
β-Mercaptoethanol	3.5 mL (100 mM)

Dissolve Tris and SDS in deionized H_2O and adjust with HCl to pH 6.7. Add the β-Mercaptoethanol and adjust the volume to 500 mL.

d. DNA Electrophoresis Solutions

50x TAE Buffer

Tris base	242 g
Glacial acetic acid	57.1 mL
0.5 M EDTA (pH 8.0)	100 mL

Loading Buffer (LB)

Bromophenol blue	0.25%
Glycerol	30%

e. Alkaline Lysis Solutions

Solution I

Glucose	50 mM
Tris-HCl	25 mM (pH 8.0)
EDTA	10 mM

Store at 4°C.

Solution II

NaOH	0.2 M
SDS	1%

Solution III

5 M KAc	60 mL
Glacial Acetic Acid	11.5 mL
H_2O	28.5 mL

Store at 4°C.

II. Plasmids

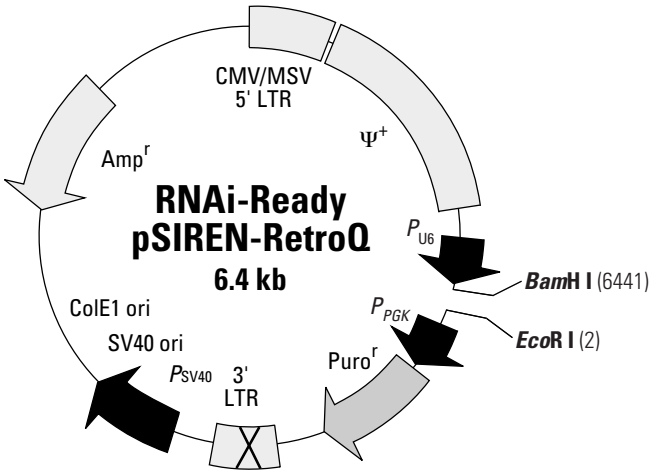

Restriction map of **RNAi-Ready pSIREN-RetroQ** Retroviral Vector. Self-inactivating retroviral expression vector designed to express shRNA. It has a human P6 promoter (PU6) and an E. coli ampicillin resistance gene.

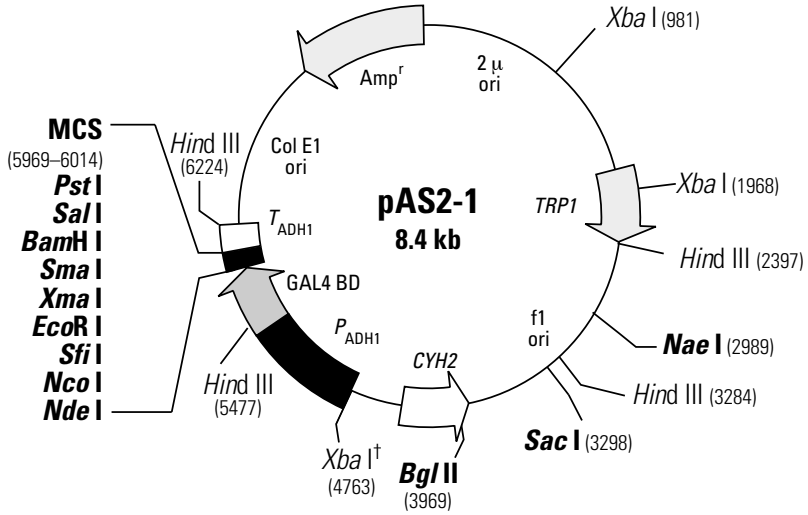

Restriction map for **pAS2-1**. Yeast two-hybrid vector pAS2-1 has an E. coli ampicillin resistance gene and restriction sites for *EcoRI* and *BamHI*.

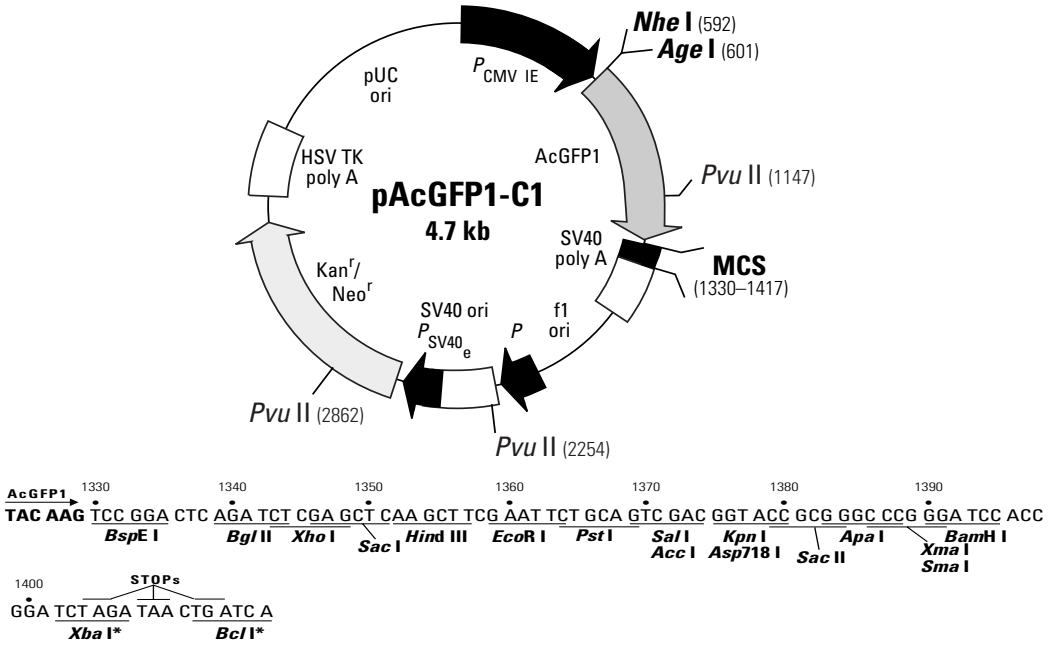

Restriction map and multiple cloning site of **pAcGFP1-C1**. pAcGFP1-C1 encodes a protein that emits green fluorescence. It contains an *E. coli* kanamycin resistance gene and has restriction sites for *EcoRI* and *BamHI* in the MCS.

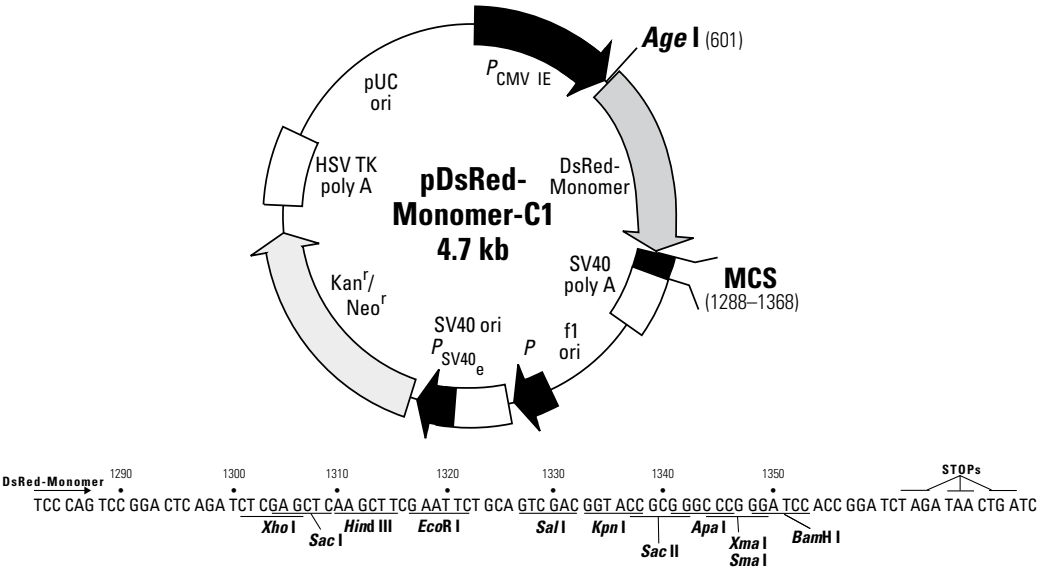

Restriction map and multiple cloning site of **pDsRed-Monomer-C1**. pDsRed-Monomer-C1 encodes a protein that emits red fluorescence. It contains an E. coli kanamycin resistance gene and has restriction sites for *EcoRI* and *BamHI* in the MCS.

III. Primers

Primer	Sequence 5'---3'	MT °C
PP1α EcoC1 FW	GGAATTCCATGTCCGACAGCGAG	60.7
PP1α BamC1 RV	CGGGATCCCTATTTCTTGGCTTT	58.0
PP1γ EcoC1 FW	GGAATTCCATGGCGGATTTAGAT	56.0
PP1γ1 BamC1 RV	CGGGATCCCTATTTCTTTGCTTG	57.8
PP1γ2 BamC1 FW	CGGGATCCTCACTCGTATAGGAC	58.8